A NEIGHBORING OPTIMUM FEEDBACK CONTROL SCHEME BASED ON ESTIMATED TIME-TO-GO WITH APPLICATION TO RE-ENTRY FLIGHT PATHS

by

Jason L. Speyer & Arthur E. Bryson, Jr.

June 1967

Technical Report No. 527

Division of Engineering and Applied Physics

Harvard University • Cambridge, Massachusetts

The suggestion for using such a scheme was first given by Kelley [4] who used performance index-to-go as the index variable. He called this a "transversal comparison" scheme. Time-to-go has the advantage that it always decreases monotonically whereas this is not always true of performance index-to-go. A monotonically changing index variable must be used if the transversal comparisons are to be made over the entire flight. The transversal comparison is used here in an iterative scheme to predict the time-to-go. Kelley's suggestion is also extended to include non-stationary systems and in-flight changes in the terminal constraints.

A NEIGHBORING OPTIMUM FEEDBACK CONTROL SCHEME BASED ON ESTIMATED TIME-TO-GO WITH APPLICATION TO RE-ENTRY FLIGHT PATHS[†]

Jason L. Speyer and Arthur E. Bryson, Jr.

Division of Engineering and Applied Physics

Harvard University   Cambridge   Massachusetts

ABSTRACT

A modification of the perturbation feedback control scheme of Refs. [1], [2], and [3] is presented that greatly increases its capability to handle disturbances in cases where the final time is not specified. The modified control scheme uses a set of precalculated gains which allows in-flight estimation of the change in the final time due to perturbations from a nominal path. The time-to-go, determined from the predicted change in final time, is used to enter tables of precalculated feedback control gains.

This modified guidance scheme is applied to a re-entry glider entering the atmosphere of the Earth at supercircular velocities. Beginning at the bottom of the pull-up maneuver (nominal altitude 188,000 ft., nominal velocity 33,000 ft./sec.$^{-1}$) the glider is guided to a terminal altitude of 220,000 ft. and zero (0) flight path angle with maximum terminal velocity. For initial altitudes between 167,000 and 216,000 ft. the terminal error in altitude is less than two feet; for initial velocities between 23,000 ft./sec. and 43,000 ft./sec. the terminal altitude error is less than 13 ft. In addition, the terminal velocity is very close to optimal for these initial conditions.

A NEIGHBORING OPTIMUM FEEDBACK CONTROL

SCHEME BASED ON ESTIMATED TIME-TO-GO WITH APPLICATION

TO RE-ENTRY FLIGHT PATHS

By

Jason L. Speyer and Arthur E. Bryson, Jr.

Technical Report No. 527

June 1967

Division of Engineering and Applied Physics

Harvard University   Cambridge, Massachusetts

1. INTRODUCTION

Among the many feedback control schemes valid for small perturbations about a nominal path is the neighboring optimum control scheme [1], [2]. This scheme generates a path neighboring to a nominal optimal path which minimizes the performance index to second order while meeting the terminal constraints. The control perturbation from the nominal control is a linear combination of the state variable perturbations weighted by a precalculated set of gains. The gains are determined by solving what is called the "accessory minimum problem" in the calculus of variations. Where more than one terminal condition is specified, some of the gains become infinite at the nominal terminal time.

The precalculated gains are conveniently stored as a function of time. Due to unforeseen disturbances, the system may not pass through the nominal initial state at the nominal initial time. The optimal path from this neighboring initial state may very well intersect the terminal manifold at a time later than the nominal terminal time; if clock time is used to enter the gain tables, the gains would become unbounded before reaching the terminal manifold. This difficulty is avoided if the gain tables are entered at an "index time" determined, so that the time-to-go on the neighboring path is the same as the time-to-go for the nominal path, i.e.,

$$(t_f - t) = (t_f^N - t_I) = \text{time-to-go} \tag{1}$$

where t_f is the estimated terminal time of the neighboring path, t_f^N is the terminal time of the nominal path, t is the clock time and t_I is the index time. As the time-to-go goes to zero the gains go to infinity

at the terminal time of the neighboring path. The time-to-go can be esti-
mated from inflight conditions by using (1) as

$$t_f - t_f^N = t - t_I \ .$$

(2)

The change in the final time, $t_f - t_f^N$, can be calculated in terms of the
deviation in the state variables from their nominal values using an additional
set of precalculated gains (see e.g., Ref. 2). This additional set of gains,
while adding some complexity, allows the control scheme to meet the terminal
constraints and achieve the minimum value of the performance index with <u>much</u>
greater perturbations from the nominal state.

2. GENERAL DESCRIPTION OF CONTROL SCHEME

The system to be controlled is described by a set of first-order non-
linear differential equations

$$\dot{x} = f(x,u,t)$$

(3)

where x is a column vector of n state variables, f is a column vector
of n known functions, u is a control vector of m control variables, t
is the independent variable time and $(\dot{\ }) \equiv d(\ )/dt$.

Control programs, $u^N(t)$, and associated state variable programs,
$x^N(t)$, are precalculated to produce a path starting from a given initial
point $x(t_o)$ that minimizes a performance index

$$J = \phi\left[x(t_f),\ t_f\right]$$

(4)

while satisfying terminal constants

$$\psi\left[x(t_f), \; t_f\right] \; = \; 0 \qquad\qquad\qquad (5)$$

where ψ is a column vector of q known functions $(q \leq n-1)$, and t_f is the (unspecified) terminal value of the independent variable.

For small variations in the state from the nominal state, a control program can be found which generates an optimum path neighboring to the nominal path. The required control perturbations, as shown in Refs. [1] and [2], may be obtained by multiplying the state deviations by a precalculated gain matrix, $\Lambda(t)$:

$$u(t) \; - \; u^N(t) \; = \; -\Lambda(t)\left[x(t) \; - \; x^N(t)\right] \; . \qquad\qquad (6)$$

To meet the constraints (5), some elements of the gain matrix, $\Lambda(t)$, may become infinite at the terminal time. If the neighboring path reaches the terminal manifold later than the nominal path, the control variation of (6) becomes undefined.

To avoid this difficulty it is suggested that the gain tables be entered at an index time determined so that the time-to-go on the nominal path is the same as the time-to-go on the neighboring path as expressed in (1). The inflight estimate of the change in the terminal time (2) is found in terms of the deviations in the state variables from the nominal values weighted by a set of precalculated gains, $K(t)$, (see Section 3 or Ref. [2]), as

$$t_f \; - \; t_f^N \; = \; t \; - \; t_I \; = \; K(t)\left[x(t) \; - \; x^N(t)\right] \; . \qquad\qquad (7)$$

Since $K(t)$, as well as $\Lambda(t)$, are calculated along the nominal, $t_f - t_f^N$ is undefined for values of t greater than t_f^N. However, instead of (7) an

implicit equation for the index time is found by using the first-order approximation

$$\left[x(t) - x^N(t)\right] = \left[x(t) - x^N(t_I)\right] - \dot{x}^N(t_I)\left[t - t_I\right] \tag{8}$$

in (7) to obtain

$$t - t_I = \frac{K(t_I)\left[x(t) - x^N(t_I)\right]}{1 + K(t_I)\dot{x}^N(t_I)} \tag{9}$$

If t and the current state vector, $x(t)$, are known, the index time can be determined rapidly by successive substitutions into (9), using tables of $K(t_I)/\left[1 + K(t_I)\dot{x}^N(t_I)\right]$ and $x^N(t_I)$.

Using Eqs. (6), (8), and $u^N(t) = u^N(t_I) + \dot{u}^N(t_I)(t-t_I)$, the control $u(t)$ may be expressed in terms of $u^N(t_I)$, $x^N(t_I)$, t_I and feedback control gains, $\Lambda(t_I)$:

$$u(t) = u^N(t_I) - \Lambda(t_I)\left[x(t) - x^N(t_I)\right]$$
$$+ \left[\Lambda(t_I)\dot{x}^N(t_I) + \dot{u}^N(t_I)\right]\left[t - t_I\right] \tag{10}$$

Note, $x(t)$ is the current estimate of the state vector and t is the clock time. If the system being controlled is stationary, that is, if the equations of motion and the boundary conditions are not explicitly dependent on time, it will be shown that

$$\left[\dot{u}^N + \Lambda(t_I)\dot{x}^N(t_I)\right] = 0 \tag{11}$$

Thus the control for a neighboring path for the stationary case is independent of the time variation $t - t_I$:

$$u(t) = u^N(t_I) - \Lambda(t_I)\left[x(t) - x^N(t_I)\right] \tag{12}$$

In the following section $\Lambda(t)$ and $K(t)$ are found by solving the accessory minimum problem in the calculus of variations. The iterative procedure for finding t_I will be eliminated by developing a gain associated with $(t-t_I)$. Also the gain matrix associated with $(t-t_I)$ in (10) is calculated through numerical integration. The need for numerical differentiation to find $\dot{u}^N(t)$ is eliminated.

3. THE ACCESSORY MINIMUM PROBLEM

The feedback gains used to estimate small changes in the control variable and final time are found by solving the accessory minimum problem (see e.g., Ref. [2] or [5]). About a stationary path (a path satisfying first-order necessary conditions) the performance index expanded to second order is minimized subject to linear dynamics. The state space for this accessory problem is composed of the deviations in the state variables away from the nominal values.

The augmented performance index for the general problem stated in the last section is defined as

$$\hat{J} = \Phi + \int_{t_o}^{t_f} \left[H(x,u,\lambda,t) - \lambda^T \dot{x} \right] dt \tag{13}$$

where

$$\Phi = \phi\left[x(t_f),\ t_f \right] + \nu^T \psi\left[x(t_f),\ t_f \right] \tag{14}$$

$$H = \lambda^T f\left[x(t),u,t \right] \tag{15}$$

Here, λ and ν are vector Lagrange multipliers associated with (3), and

(5), respectively. The initial and final times are t_o and t_f. The Euler-Lagrange necessary conditions are

$$\dot{\lambda} = -H_x \tag{16}$$

$$H_u = 0 \tag{17}$$

The terminal conditions are

$$\lambda(t_f) = \Phi_x \tag{18}$$

$$\Omega = H + \Phi_t = 0 \tag{19}$$

where $(\ )_x$ means $\partial(\ )/\partial x$.

In the accessory minimum problem, $\delta u(t)$ is to be determined which minimizes the second-order expansion of the augmented performance index (13)

$$d^2\hat{J} = \frac{1}{2}\left\{ [\delta x^T, d\nu^T, dt_f] \begin{bmatrix} S & R & m \\ R & Q & n \\ m^T & n^T & \alpha \end{bmatrix} \begin{bmatrix} \delta x \\ d\nu \\ dt_f \end{bmatrix} \right\}_{t=t_f} + \frac{1}{2}\int_{t_o}^{t_f} [\delta x^T \delta u^T] \begin{bmatrix} H_{xx} & H_{xu} \\ H_{ux} & H_{uu} \end{bmatrix} \begin{bmatrix} \delta x \\ \delta u \end{bmatrix} dt \tag{20}$$

subject to

$$\dot{\delta x} = f_x \delta x + f_u \delta u \tag{21}$$

$$\delta x(t_o) \quad \text{specified} \tag{22}$$

$$d\psi = \psi_x \delta x + \dot{\psi}dt_f \quad \text{where} \quad d\psi \text{ is specified} \tag{23}$$

where the deviation in any variable Q is defined as

$$\delta Q = Q(t) - Q^N(t) \tag{24}$$

The weighting matrix in (20) is

$$
\begin{bmatrix} S & R & m \\ R^T & Q & n \\ m^T & n^T & \alpha \end{bmatrix}_{t=t_f} = \begin{bmatrix} \phi_{xx} & \phi_{x\nu} & \dfrac{d}{dt_f}\left[\phi_x\right]-\phi_x f_x \\[2ex] \phi_{\nu x} & \phi_{\nu\nu} & \dfrac{d}{dt_f}\left[\phi_\nu\right] \\[2ex] \left[\dfrac{d}{dt_f}\phi\right]_x & \left[\dfrac{d}{dt_f}\phi\right]_\nu & \dfrac{d}{dt_f}\left[\dfrac{d}{dt_f}\phi\right] \end{bmatrix} \tag{25}
$$

Note that this matrix is symmetric.

First-order necessary conditions for the accessory minimum problem may be developed as follows. Define the variational Hamiltonian for this accessory problem as

$$
\Delta H = \frac{1}{2}\left\{\begin{bmatrix}\delta x^T, \delta u^T\end{bmatrix}\begin{bmatrix} H_{xx} & H_{xu} \\ H_{ux} & H_{uu} \end{bmatrix}\begin{bmatrix}\delta x \\ \delta u\end{bmatrix}\right\} + \delta\lambda^T\left[f_x \delta x + f_u \delta u\right] \tag{26}
$$

the necessary conditions are

$$
\dot{\delta x} = (\Delta H)_{\delta\lambda} \tag{27}
$$

$$
\dot{\delta\lambda} = -(\Delta H)_{\delta x} \tag{28}
$$

$$
0 = (\Delta H)_{\delta u} \tag{29}
$$

From (29) the perturbed control is given in terms of δx and $\delta\lambda$ as

$$
\delta u = -H_{uu}^{-1}\left[H_{ux}\delta x + H_{u\lambda}\delta\lambda\right] \tag{30}
$$

where H_{uu} is assumed to be non-singular.

In order to develop a feedback law from (30) and predict the change

- 7 -

in terminal time from present state deviations, a linear relation among the variables δx, $d\nu$, dt_f, $\delta\lambda$, $d\psi$ and $d\Omega$, developed in Ref. [2], is presented here as

$$
\begin{bmatrix} \delta\lambda(t) \\ d\psi \\ d\Omega \end{bmatrix} = \begin{bmatrix} S(t) & R(t) & m(t) \\ R^T(t) & Q(t) & n(t) \\ m^T(t) & n^T(t) & \alpha(t) \end{bmatrix} \begin{bmatrix} \delta x(t) \\ d\nu \\ dt_f \end{bmatrix} \tag{31}
$$

The elements of the coefficient matrix of (31) are called "sweep" variables and are determined by a symmetric but non-linear differential equation (developed in Ref. [2]):

$$
\frac{d}{dt} \begin{bmatrix} S & R & m \\ R^T & Q & n \\ m^T & n^T & \alpha \end{bmatrix} = \begin{bmatrix} I_n & S \\ 0_q^T & R^T \\ 0_1^T & m^T \end{bmatrix} \begin{bmatrix} -C & -A^T \\ -A & B \end{bmatrix} \begin{bmatrix} I_n & 0_q & 0_1 \\ S & R & m \end{bmatrix} \tag{32}
$$

where

$$
A = f_x - f_u H_{uu}^{-1} H_{ux} \tag{33}
$$

$$
B = f_u H_{uu}^{-1} f_u^T \tag{34}
$$

$$
C = H_{xx} - H_{xu} H_{uu}^{-1} H_{ux} \tag{35}
$$

The boundary conditions are given by (25).

4. PROPERTIES OF SWEEP VARIABLES

The differential equations of (32) are integrated backwards from

the terminal manifold, stopping at the initial time. If there are no conjugate points $(\hat{S} \neq \infty)$ and the path is normal $(\hat{Q} < 0$ for a minimum) as defined in Ref. [5], then (30) can be manipulated into the form (on an optimal path $\Omega = 0 \implies d\Omega = 0$)

$$
\begin{bmatrix} \delta\lambda(t) \\ d\nu \\ dt_f \end{bmatrix} = \begin{bmatrix} \hat{S} & \hat{R} \\ \hat{R}^T & \hat{Q} \\ \hat{m}^T & \hat{n}^T \end{bmatrix} \begin{bmatrix} \delta x(t) \\ d\psi \end{bmatrix} \qquad \text{(36)}
$$

where

$$
\hat{S} = S - \frac{m^T}{\alpha} - \hat{R}\hat{Q}^{-1}\hat{R}^T \qquad \text{(37)}
$$

$$
\hat{Q} = \left(Q - \frac{nn^T}{\alpha} \right)^{-1} \qquad \text{(38)}
$$

$$
\hat{R} = -\left(R - \frac{mn^T}{\alpha} \right)\hat{Q} \qquad \text{(39)}
$$

$$
\hat{m} = -\hat{R}\frac{n}{\alpha} - \frac{m}{\alpha} \qquad \text{(40)}
$$

$$
\hat{n} = -\hat{Q}\frac{n}{\alpha} \qquad \text{(41)}
$$

It should be noted that these new variables, $(\hat{\ })$, still satisfy (32). This transformation is desirable in order that the perturbed control of (30) be written as a feedback law operating on the deviations of the state variables. When integrating (32), this transformation must be taken in a time interval which lies some time before the terminal boundary (corresponding to Q close to zero) and some time after a conjugate point defined for an arc with no terminal constraints on the state space but with fixed terminal time (this corresponds to S becoming unbounded). For the atmospheric re-entry guidance problem to be given in Section 7, S does go to ∞ although $\hat{S}$ remains bounded (also see Appendix C).

5. FEEDBACK GAINS

The feedback gains $K(t)$ and $\Lambda(t)$ can now be identified with the sweep variables. From (36) the general form for predicting the change in the terminal time is

$$dt_f = \hat{m}^T(t)\delta x(t) + \hat{n}^T d\psi \qquad (42)$$

where $\hat{m}^T \equiv K(t)$. This form has the additional flexibility of allowing small changes in the terminal constraints.

Instead of developing the implicit equation as (9) let us suppose that some estimate of $t-t_I$ was made. If the system has undergone a perturbation then (2) does not hold but differs by some error, ε, as

$$(t-t_I)^{NEW} = (t-t_I) + \varepsilon \quad . \qquad (43)$$

If (43) is introduced into (42) along with (8) and $(t - t_I)^{NEW} = dt_f$ an explicit equation can be obtained for calculating ε:

$$\varepsilon = \hat{m}^T(t_I)\left[x(t) - x(t_I)\right] - \ell(t_I)(t-t_I) + \hat{n}^T(t_I)d\psi \qquad (44)$$

where

$$\ell(t_I) = 1 + \hat{m}^T(t_I)f^N(t_I) \qquad (45)$$

Note that in (44) second-order terms are neglected. Equations (43)-(45) are used iteratively until $\varepsilon \cong 0$. For the numerical problem to be discussed, ε was very small within two iterations.

The index time that results from this iterative procedure is used

to enter the gain tables from which the perturbed control variable is calculated. If the linear expression for $\delta\lambda(t)$ in (36) is substituted into (30), the perturbed control is

$$\delta u \;=\; -\Lambda(t)\delta x(t) - \beta(t)d\psi \tag{46}$$

where

$$\Lambda(t) \;=\; H_{uu}^{-1}(t)\left[H_{ux}(t) + H_{u\lambda}(t)\hat{S}(t)\right] \tag{47}$$

$$\beta(t) \;=\; H_{uu}^{-1}(t)H_{u\lambda}(t)\hat{R}(t) \tag{48}$$

The control program on the neighboring path can be written as a function of index time with the help of (8):

$$u(t) \;=\; u^N(t_I) - \Lambda(t_I)\left[x(t) - x^N(t_I)\right] + r(t_I)\left[t-t_I\right] - \beta(t_I)d\psi \tag{49}$$

where

$$r(t_I) \;=\; \Lambda(t_I)f^N(t_I) + \dot{u}^N(t_I) \tag{50}$$

The control program also allows for variations in the terminal conditions. Second-order terms in (49) are neglected.

For systems which are stationary the gains ℓ and r are zero. In Appendix A the explicit dependence of these gains on time is demonstrated.

6. ANALYTIC EXAMPLE OF CONTROL SCHEME

The following example is chosen to illustrate some of the features of the previous section for non-stationary problems. The problem is to reach

a parabolic boundary in x,t space so that a combination of terminal time and integral squared velocity is minimized. This might be interpreted as a one-dimensional pursuit problem in which the target has a constant acceleration.

The problem statement is: find the control variable, u, that minimizes

$$J = \int_0^{t_f} (1+u^2)dt \tag{51}$$

with dynamical equations

$$\dot{x} = u \tag{52}$$

and the terminal boundary

$$\psi = x_f + t_f^2 - 1 = 0 \tag{53}$$

The augmented performance index is

$$\hat{J} = \phi + \int_0^{t_f} [H - \lambda\dot{x}]dt \tag{54}$$

where

$$\phi = \nu(t_f + \frac{1}{2}t_f^2 - 1) \tag{55}$$

$$H = 1 + \frac{1}{2}u^2 + \lambda u \tag{56}$$

First-order necessary conditions are

$$\dot{\lambda} = u \quad ; \quad \lambda(t_f) = \nu \tag{57}$$

$$H_u = 0 \implies u = -\lambda \tag{58}$$

$$H + \phi_t\Big|_{t=t_f} = 0 \tag{59}$$

From (57), (58), and (59) the control variable as a function of terminal

time is

$$u = -\left[t_f - (t_f^2 + 2)^{1/2}\right] \tag{60}$$

Using the dynamic equation (52) the relation between the initial state and terminal time is

$$x_o = 1 + t_f\left[\frac{t_f}{2} - (t_f^2 + 2)^{1/2}\right] \tag{61}$$

Choosing x_o and solving for t_f the performance index can be evaluated using (51) and (60) as

$$J = 2 + t_f^2 - t_f(t_f^2 + 2)^{1/2} \tag{62}$$

The optimal paths for different initial conditions are plotted in Fig. 1. Note that the control variable along each of these paths is different. These paths terminate on the parabolic manifold in x, t space. Lines of constant time-to-go (dashed lines) and constant performance index (dashed dotted lines) are super-imposed on the trajectories. Suppose that the control scheme of the last section is applied to this problem. Consider that the path emanating from $x = .4$, $t = 0$ is the nominal path. Now at $t = .32$ the state $x = .3$ is measured. If present time is used as the index time, then the nominal value of the state would be $x^N = .7$. As t approaches $t = .5$, the nominal path meeds the terminal manifold. From this point on, the control on the neighboring path is not defined since no gains are calculated beyond this point. However, if the index time is chosen so that the time-to-go to the terminal boundary for both the neighboring path and nominal path are the same, the gain tables of the nominal are entered when $x^N = .4$ and $t = 0$. As time progresses, both paths reach the terminal boundary together.

Note that if two paths start at the same position but at different times the optimal controls for each resulting optimum path are not the same. This difference in time between the present time and index time for non-stationary problems must explicitly be included in the calculation of the control deviation as given by (10).

The control gains for calculating the perturbed control and predicting the error in the difference of the times-to-go are easily found from the scheme of the last section and are given here as

$$\epsilon = \left[\frac{u^N + t_f^N}{u^N(t_f^N - t_I) - (u^N + t_f^N)^2} \right] \left[x(t) - x^N(t_I) \right] + \left[\frac{u^N t_I + (t_f^N)^2}{u^N(t_f^N - t_I) - (u^N + t_f^N)^2} \right] (t - t_I) \quad (63)$$

$$u(t) - u^N(t_I) = \left[\frac{-u^N}{u^N(t_f^N - t_I) - (u^N + t_f^N)^2} \right] \left[x(t) - x^N(t_I) \right] + \left[\frac{(u^N)^2}{u^N(t_f^N - t_I) - (u^N + t_f^N)^2} \right] (t - t_I) \quad (64)$$

7. NUMERICAL EXAMPLE:

GUIDANCE SCHEME FOR A RE-ENTRY GLIDER

The control scheme is applied here to the problem of guiding a lifting re-entry vehicle at supercircular velocities from the bottom of the pull-up maneuver (nominal altitude 188,000 ft., nominal velocity 33,000 ft.sec.$^{-1}$, nominal flight path angle $-0.1°$) to an altitude of 220,000 ft. at zero flight path angle while maximizing the terminal velocity.[†] This minimizes the energy loss at the terminal altitude. The nomenclature for this problem is given in

---

[†] This starting point was chosen to save computer time. Usually control begins at entry into the atmosphere (altitude = 400,000 ft.) as in Ref. [1]. Note that from the entry point the performance index, velocity, is <u>not</u> monotonically decreasing.

- 14 -

Fig. 2. The aerodynamic forces, lift and drag, are varied through the control variable, angle-of-attack $\alpha(t)$. The wing loading of the vehicle, mg_o/S, was taken as 61.3 lb.ft.$^{-2}$. The 1956 ARDC standard atmosphere model was used. The lift-drag characteristics of the vehicle are shown in Fig. 3. The non-linear equations of motion of a point mass about a spherical non-rotating Earth are given in Appendix B. The state variable histories for the nominal optimal path are given in Fig. 4.

This problem is stationary and as such is independent of the starting time. Therefore, the nominal may be thought of as shifted in time so that the terminal time of the nominal is the same as that of the neighboring path. This again causes the time-to-go on both paths to be the same. The gains for the continuous in-flight prediction of the error in time-to-go is given by K_v^t, K_γ^t, K_h^t tablulated in Fig. 4 where

$$\epsilon = K_v^t(t_I)\left[v(t)-v^N(t_I)\right] + K_\gamma^t(t_I)\left[\gamma(t)-\gamma^N(t_I)\right] + K_h^t(t_I)\left[h(t)-h^N(t_I)\right] \qquad (65)$$

The index time, t_I, is found so that $\epsilon = 0$ by the procedure of Sect. 5. Once t_I is found the perturbed value of angle-of-attack is calculated using the feedback gains K_v^α, K_γ^α, K_h^α tabulated in Fig. 4 as

$$\alpha(t) - \alpha^N(t_I) = K_v^\alpha(t_I)\left[v(t) - v^N(t_I)\right] + K_\gamma^\alpha(t_I)\left[\gamma(t)-\,^N(t_I)\right]$$
$$+ K_h^\alpha(t_I)\left[h(t) - h^N(t_I)\right] \qquad (66)$$

The first-order necessary conditions and coefficient matrices for the sweep equations for this problem are given in Appendix B.

The feedback gains tabulated in Fig. 4 are seen to be positive at the beginning of the flight and then go to negative values. This same

behavior occurs in guiding a vehicle to a fixed point along the minimum distance path on the surface of a sphere (see Appendix C). Positive feedback for the re-entry problem is required to maximize the velocity whereas negative feedback is required to meet the terminal constraint. Near the end of the flight the guidance scheme concentrates on meeting the terminal constraints, whereas with time-to-go large, it concentrates on maximizing terminal velocity.

The modified control scheme which uses time-to-go all along the path is compared with the control scheme which uses present time as the index time (this is the same control scheme used in Ref. [1]). The control schemes are tested by introducing variations first in the altitude and then in the velocity. Figure 5 shows trajectories in altitude-velocity space generated by the modified control scheme for initial altitudes between 176,000 ft. and 216,000 ft. all with initial velocity = 33,100 ft.sec.$^{-1}$ and initial γ = -0.10^{o}. Plotted also on this chart are constant time-to-go curves. For paths resulting from positive initial altitude perturbations, the estimated time-to-go is shorter than the nominal time-to-go. Thus, the gains used were larger negative values for this index time than they would have been if nominal time-to-go had been used to enter the gain tables. For trajectories initialized by h = 216,000 ft. the path reaches the terminal point in less than half the nominal time. Prediction of the perturbed terminal time was very good. The angle-of-attack programs for two paths with large initial altitude variations are shown with the nominal α-program in Fig. 6. In the altitude-velocity space of Fig. 7, a family of trajectories generated by the modified control scheme are shown for initial velocities between

23,000 ft./sec. and 46,000 ft./sec.

The errors in final altitude when the flight path angle is zero are shown in Fig. 8 for variations in initial altitude and in Fig. 9 for variations in initial velocity. For the scheme based on clock time large errors are incurred; for $\delta h(t_o) = 16,000$ ft., the terminal altitude error is 1400 ft. (Fig. 7) and for $\delta v(t_o) = 6,000$ ft./sec. the terminal altitude error is 2400 ft. For the range of initial altitudes and velocities given earlier for the modified scheme, Fig. 8 indicates the terminal altitude error is less than 3 ft. and Fig. 9 also indicates small altitude errors except for large initial variations in velocity such as 13,000 ft./sec. where the error is 93 ft.

Not only does the modified scheme meet the terminal constraints on $\gamma(t_f)$ and $h(t_f)$ better but it also achieves greater terminal velocity. A comparison in terminal velocity between the control scheme based on clock time, the modified control scheme and the first-order approximation relating changes in the terminal velocity to changes in the initial conditions (the adjoint variable) is shown in Fig. 10 for variations in initial altitude and in Fig. 11 for variations in initial velocity. The greatest improvement made by the modified control is for $\delta h(t_o) < 0$ and $\delta v(t_o) < 0$. It is for these variations that the scheme based on clock time "runs" out of gains and uses the largest α available ($\pm$ 60 DEG). However, the modified scheme does better in maximizing the velocity for all variations. Note that the terminal velocity of the modified scheme lies very close to the first-order approximation.

8. COMMENTS ON EXTENSIONS OF THE NUMERICAL EXAMPLE

If the guidance scheme is initialized at entry into the atmosphere, the velocity first increases and then decreases. This makes it impossible to use velocity-to-go as an index variable as proposed in Ref. 4 . However, in the region where velocity is monotonically decreasing the number of gains can be reduced by one if velocity-to-go is used as the index variable instead of time. The dynamics are velocity dependent; i.e., non-stationary with respect to velocity. The gains ℓ and r of (45) and (50) are non-zero and can be easily calculated from the now 2-vectors, $\hat{m}$, f and Λ.

The gains r and ℓ would be also non-zero if the boundary conditions were explicit functions of time. This would occur if the terminal positions were constrained and the rotation of the Earth included.

9. CONCLUSIONS

The performance of the re-entry guidance scheme demonstrates that using time-to-go as the index variable over the entire path increases greatly the range of possible initial conditions while still meeting the terminal conditions and achieving the maximum value of performance. The appropriate gain to choose depends upon the estimated flight time to the terminal boundary, not the clock time.

The range of initial conditions handled is so great that, in general, only one reference nominal would have to be stored on an on-board computer to guide a re-entry vehicle. Even further savings in storage may be gained by storing only the coefficients of a polynomial fit to the reference path

and gains. For gains that have singularities at the terminal point it is suggested the polynomial also have a singular term proportional to some power of $(t_f-t)^{-1}$.

ACKNOWLEDGMENTS

REFERENCES

[1]   Breakwell, J., Speyer, J. L., and Bryson, A. E. Jr., "Optimization and Control of Nonlinear Systems Using the Second Variation," J. SIAM on Control 1, No. 2 (1963).

[2]   McReynolds, S. R., and Bryson, A. E. Jr., "A Successive Sweep Method for Solving Optimal Programming Problems," Sixth Joint Automatic Control Conference, Troy, New York, June 1965.

[3]   Mitter, S. K., "Successive Approximation Method for the Solution of Optimal Control Problems," Automatica 3, 135-149 (1966).

[4]   Kelley, H., "An Optimal Guidance Approximation Theory," IEEE Trans. AC-9, 375-380 (1964).

[5]   Bryson, A. E. Jr., and Ho, Y. C., Optimization, Estimation, and Control, Lecture Notes, Harvard University, 1967.

APPENDIX A

Feedback Gains on $(t-t_I)$

A geometrical interpretation of the sweep variables is given through a Hamilton-Jacobi viewpoint as presented in Ref. [2]. An optimal return function, $V(x,t,\psi)$, is defined as the value of $\hat{J}$ of (15) when starting from x at time $t \leq t_f$ keeping $H_u = 0$ along the path and meeting terminal constraints ψ with $\Omega = 0$. For small variations in x,ψ and Ω the sweep and adjoints variables can be interpreted in terms of the optimal return function as

$$\lambda^T(t) = V_{x(t)} \tag{A-1}$$

$$\hat{S}(t) = V_{x(t)x(t)} \tag{A-2}$$

$$\hat{R}(t) = V_{\psi x(t)} \tag{A-3}$$

$$\hat{Q}(t) = V_{\psi\psi} \tag{A-4}$$

$$\hat{m}(t) = V_{\Omega x(t)} \tag{A-5}$$

$$\hat{n}(t) = V_{\Omega\psi} \tag{A-6}$$

$$\hat{\alpha}(t) = V_{\Omega\Omega} \tag{A-7}$$

The partials are implied by the expansions of (36).

Using the above identifications the explicit dependence of the gain r in (50) on time is illustrated. Also an alternative scheme for calculating r is given where $\dot{u}^N$ need not be calculated by numerical differentiation on the computer. The expression for Λ given by (47) in terms of the return function is

$$\Lambda = H_{uu}^{-1}\left[V_x f_{ux} + f_u^T V_{xx}\right] \tag{A-8}$$

From $\dot{H}_u = 0$ the value of $\dot{u}$ along an optimal path is

$$\dot{u} = -H_{uu}^{-1}\left[V_x f_{ux} f + V_x f_{ut} + \frac{d}{dt}(V_x) f_u\right] \tag{A-9}$$

where

$$\frac{d}{dt}(V_x) = V_{xx} f + V_{xt} \tag{A-10}$$

Note that the order of total and partial differentiation is important.
Introducing (A-8) and (A-9) into the expression for (50) gives

$$r = H_{uu}^{-1}\left[V_x f_{ut} + V_{tx} f_u\right] = H_{uu}^{-1}\left[V_x f_u\right]_t \tag{A-11}$$

If $V_x f_u$ is not explicitly dependent upon time $r = 0$ and the neighboring
control program is stationary. Note that $\dot{u}$ of (A-9) is easily calculated
by using

$$\frac{d}{dt}(V_x) = -V_x f_x \tag{A-12}$$

where V_x is identified as the adjoint in (A-1).

The dependency of the gain ℓ on t is demonstrated directly once
$\delta x = dx - f dt$ is used in (36). The change in the terminal time is then
related to a change in the present time as

$$dt_f = \hat{m}^T dx - \hat{m}^T f dt + \hat{n}^T d\psi \tag{A-13}$$

The term $\hat{m}^T f$ is seen to be $-\partial t_f/\partial t$ keeping x, ψ and Ω constant. Then
ℓ defined by (45) is

$$\ell = \left[1 - \frac{\partial t_f}{\partial t}\right] \tag{A-14}$$

A stationary problem depends only on the time interval and not on a particular value. Thus if the problem is begun a time dt late, it will finish a time dt late. That is $\partial t_f/\partial t = 1$ which in turn implies that $\ell \equiv 0$ for stationary problems. To calculate ℓ in terms of partials of the return function with respect to t, time may be regarded as a state variable and the index time t_I be the independent variable. Since the problem is not explicitly dependent on the new variable t_I, the indexing variable t_I is found by entering the gain tables so that the predicted value of the change in the terminal value of t_I is zero. This is equivalent to nulling ϵ.

APPENDIX B

Equations Used in the Atmospheric Re-entry Problem

The equations of motion for a re-entry vehicle about a non-rotating spherical Earth are

$$\dot{V} = -\frac{C_D \rho V^2 S}{2m} - g \sin\gamma \tag{B-1}$$

$$\dot{\gamma} = \frac{C_L \rho V S}{2m} + \left(\frac{V}{R+h} - \frac{g}{V}\right) \cos\gamma \tag{B-2}$$

$$\dot{h} = V \sin\gamma \tag{B-3}$$

where V, γ, h is the state vector and t = time is the independent variable. The variational Hamiltonian is

$$H = -\lambda_V \left[\frac{C_D \rho V^2 S}{2m} + g \sin\gamma\right] + \lambda_\gamma \left[\frac{C_L \rho V S}{2m} + \left(\frac{V}{R+h} - \frac{g}{V}\right)\cos\gamma\right] \tag{B-4}$$

$$+ \lambda_h \left[V \sin\gamma\right]$$

The Euler-Lagrange equations are

$$\dot{\lambda}_V = -H_V = \frac{C_D \rho V S}{m} \lambda_V - \left[\frac{C_L \rho S}{2m} + \left(\frac{1}{R+h} + \frac{g}{V^2}\right)\cos\gamma\right]\lambda_\gamma - \sin\gamma \, \lambda_h \tag{B-5}$$

$$\dot{\lambda}_\gamma = -H_\gamma = g\cos\gamma \, \lambda_V + \left(\frac{V}{R+h} - \frac{g}{V}\right)\sin\gamma \, \lambda_\gamma - V\cos\gamma \, \lambda_h \tag{B-6}$$

$$\dot{\lambda}_h = -H_h = \left[-\frac{2g}{R+h}\sin\gamma + \frac{C_D V^2 S}{2m}\frac{\partial\rho}{\partial h}\right]\lambda_V + \left[\left(\frac{V}{(R+h)^2} - \frac{2g}{V(R+h)}\right)\cos\gamma\right.$$

$$\left. - \frac{C_L V S}{2m}\frac{\partial\rho}{\partial h}\right]\lambda_\gamma \tag{B-7}$$

The partials of the Hamiltonian needed to evaluate the matrices A, B, and

C of (33), (34), and (35) are

$$H_{vv} = -\lambda_v \left[\frac{C_D \rho S}{m} \right] - \lambda_\gamma \left[\frac{2g}{V^3} \cos\gamma \right] \tag{B-8}$$

$$H_{v\gamma} = - \lambda_\gamma \left(\frac{1}{R+h} + \frac{g}{V^2} \right) \sin\gamma + \lambda_h \cos\gamma \tag{B-9}$$

$$H_{vh} = - \frac{\lambda_v C_D VS}{m} \frac{\partial\rho}{\partial h} + \left[\frac{C_L S}{2m} \frac{\partial\rho}{\partial h} - \frac{\cos\gamma}{(R+h)^2} - \frac{2g \cos\gamma}{V^2(R+h)} \right] \lambda_\gamma \tag{B-10}$$

$$H_{\gamma\gamma} = \lambda_v g \sin\gamma - \lambda_\gamma \left(\frac{V}{R+h} - \frac{g}{V} \right) \cos\gamma - \lambda_h V \sin\gamma \tag{B-11}$$

$$H_{\gamma h} = \lambda_v \frac{2g}{(R+h)} \cos\gamma + \lambda_\gamma \left(\frac{V}{(R+h)^2} - \frac{2g}{V(R+h)} \right) \sin\gamma \tag{B-12}$$

$$H_{hh} = -\lambda_v \left[\frac{C_D V^2 S}{2m} \frac{\partial^2\rho}{\partial h^2} + \frac{6g}{(R+h)^2} \sin\gamma \right] + \lambda_\gamma \left[\frac{C_L VS}{2m} \frac{\partial^2\rho}{\partial h^2} \right.$$
$$\left. + \frac{2V}{(R+h)^3} \cos\gamma - \frac{6g}{V(R+h)^2} \right] \tag{B-13}$$

$$H_{v\alpha} = -\lambda_v \frac{\rho VS}{m} \frac{\partial C_D}{\partial\alpha} + \lambda_\gamma \frac{\rho S}{2m} \frac{\partial C_L}{\partial\alpha} \tag{B-14}$$

$$H_{\gamma\alpha} = 0 \tag{B-15}$$

$$H_{h\alpha} = - \frac{\lambda_v V^2 S}{2m} \frac{\partial\rho}{\partial h} \frac{\partial C_D}{\partial\alpha} + \lambda_\gamma \frac{VS}{2m} \frac{\partial\rho}{\partial h} \frac{\partial C_L}{\partial\alpha} \tag{B-16}$$

$$H_{\alpha\alpha} = -\lambda_v \frac{\rho V^2 S}{2m} \frac{\partial^2 C_D}{\partial\alpha^2} + \lambda_\gamma \frac{\rho VS}{2m} \frac{\partial^2 C_L}{\partial\alpha^2} \tag{B-17}$$

$$H_{\lambda_v\alpha} = - \frac{\rho V^2 S}{2m} \frac{\partial C_D}{\partial\alpha} \tag{B-18}$$

$$H_{\lambda_\gamma}\alpha = \frac{\rho VS}{2m}\frac{\partial C_L}{\partial \alpha} \qquad \text{(B-19)}$$

$$H_{\lambda_h}\alpha = 0 \qquad \text{(B-20)}$$

$$H_{\lambda_V}V = -\frac{C_D\rho VS}{m} \qquad \text{(B-21)}$$

$$H_{\lambda_\gamma}V = \frac{C_L\rho S}{m} + \left(\frac{1}{R+h} + \frac{g}{V^2}\right)\cos\gamma \qquad \left.\right\} f_V \qquad \text{(B-22)}$$

$$H_{\lambda_h}V = \sin\gamma \qquad \text{(B-23)}$$

$$H_{\lambda_V}\gamma = -g\,\cos\gamma \qquad \text{(B-24)}$$

$$H_{\lambda_\gamma}\gamma = -\left(\frac{V}{R+h} - \frac{g}{V}\right)\cos\gamma \qquad \left.\right\} f_\gamma \qquad \text{(B-25)}$$

$$H_{\lambda_h}\gamma = V\,\cos\gamma \qquad \text{(B-26)}$$

$$H_{\lambda_V}h = -\frac{C_D V^2 S}{2m}\frac{\partial\rho}{\partial h} + \frac{2g\,\sin\gamma}{R+h} \qquad \text{(B-27)}$$

$$H_{\lambda_\gamma}h = \frac{C_L VS}{2m}\frac{\partial\rho}{\partial h} - \left(\frac{V}{(R+h)^2} - \frac{2g}{V(R+h)}\right)\cos\gamma \qquad \left.\right\} f_h \qquad \text{(B-28)}$$

$$H_{\lambda_h}h = 0 \qquad \text{(B-29)}$$

- 25 -

APPENDIX C

Character of the Feedback Control Gains

The feedback control gains for the optimal guidance scheme of a re-entry vehicle have positive values at the beginning of the flight and become negative toward the end of the flight (see Fig. 4). The same behavior is found for the control gains in guiding a vehicle along the shortest path to a fixed point on a sphere (Ref. [5]). Spherical coordinates are used as defined in Fig. 12. The element of distance, ds, on the surface of the sphere is

$$ds = r\left[(d\theta)^2 + \cos^2\theta (d\phi)^2\right]^{1/2} \tag{C-1}$$

where r = radius of the sphere. The problem is to find $u(\phi)$ to minimize

$$J = \int_0^{\phi_1} \left[u^2 + \cos^2\theta\right]^{1/2} d\phi \tag{C-2}$$

where

$$\frac{d\theta}{d\phi} = u$$

$$\theta(0) = 0 \quad , \quad \theta(\phi_1) = 0$$

The method of solution for this problem will be to solve the accessory minimum problem using the Riccati equation approach given in the text. Here ϕ will be the independent variable.

It is straight forward to show that $u(\phi) = 0$, $\theta(\phi) = 0$ satisfies the first-order necessary conditions. Let us consider neighboring paths by expanding the performance index (C-2) to second order as

$$\delta^2 J \;\tilde{=}\; \frac{1}{2} \int_0^{\phi_1} [u^2 - \theta^2] d\phi \qquad \text{(C-3)}$$

Here u and θ are deviations away from the nominal $u = 0$, $\phi = 0$. The Hamiltonian for the accessory minimum problem is

$$H \;=\; \frac{1}{2}[u^2 - \theta^2] + \lambda u \qquad \text{(C-4)}$$

and the Euler-Lagrange equations are

$$\frac{d\lambda}{d\phi} \;=\; -H_\theta \;, \qquad \lambda(\phi_1) = \nu \qquad \text{(C-5)}$$

$$H_u = 0 \;\Longrightarrow\; u = -\lambda \qquad \text{(C-6)}$$

where ν is a Lagrange multiplier on the terminal constraint $\theta(\phi_1) = 0$.

The Riccati transformation of (36) is used to relate λ to θ in developing the feedback law. Here for $f_x = 0$, $f_u = 1$, $H_{\theta\theta} = -1$, $H_{\theta u} = 0$, $H_{uu} = +1$, the sweep variables are determined from (32)

$$\frac{dS}{d\phi} \;=\; S^2 + 1 \quad ; \qquad S(\phi_1) = 0 \qquad \text{(C-7)}$$

$$\frac{dR}{d\phi} \;=\; SR \quad ; \qquad R(\phi_1) = 1 \qquad \text{(C-8)}$$

$$\frac{dQ}{d\phi} \;=\; R^2 \quad ; \qquad Q(\phi_1) = 0 \qquad \text{(C-9)}$$

The solutions in the interval $0 \leq \phi_1 - \phi \leq \pi/2$ are easily obtained:

$$S \;=\; -\tan(\phi_1 - \phi) \qquad \text{(C-10)}$$

$$R \;=\; \sec(\phi_1 - \phi) \qquad \text{(C-11)}$$

$$Q \;=\; -\tan(\phi_1 - \phi) \qquad \text{(C-12)}$$

Note that as $\phi_1 - \phi \to \pi/2$, S and Q go to ∞. This value of S corresponds to a problem where ϕ_1 is fixed but $\theta(\phi_1)$ is free. $S = \infty$ corresponds to a conjugate point for the unconstrained problem. If S is transformed to

that it relates to the fixed end point problem, $\theta(\phi_1) = 0$,

$$\hat{S} = S - RQ^{-1}R = ctn\left[\phi_1 - \phi\right] \qquad (C-13)$$

S, R, and Q do not exist for $(\phi_1-\phi) > \pi/2$, but $\hat{S}$ (propagated also by (C-7)) exists in the interval $0 \le \phi_1 - \phi \le \pi$ where at $(\phi_1-\phi) = 0$, $\hat{S} \to -\infty$. Note $\hat{S} \to \infty$ as $\phi_1 - \phi \to \pi$, so the latter is a conjugate point for the constrained problem. From the point $\phi = 0$, $\theta = 0$ to $\phi = \pi$, $\theta = 0$ there are an infinite number of great circles which all give the same value of the performance index. Using the Riccati transform and (C-6) the neighboring optimal feedback law is

$$u = -\hat{S}\theta \quad . \qquad (C-14)$$

The feedback gain, $-\hat{S}(\phi)$, is negative between $0 \le \phi_1 - \phi \le \pi/2$ and positive between $\pi/2 \le \phi_1 - \phi \le \pi$. For values of $\phi_1 - \phi > \pi$ the nominal path is not a minimizing path.

Consider a variation from the equatorial nominal path to the point A shown in Fig. 12. The optimum path from A to the terminal point ($\theta = 0$, $\phi = \pi$) diverges from the nominal path until $\phi = \pi/2$, then converges to the nominal path as $\phi \to \pi$. Consider an airplane flying eastward along the equator to a destination on the equator. If a disturbance moves the airplane north of the equator when there is more than 90° to go to its destination, it should change its flight path to slightly north of east (positive feedback). If there were less than 90° to go, it should change its flight path to slightly south of east (negative feedback). Using the feedback law of (C-14), a control is found initially which forces the neighboring path further from the nominal path. The slope of the neighboring path in the direction away from the nominal is an effort to minimize the

performance index. This corresponds to positive feedback in (C-14).
However, after the median $\phi = \pi/2$ is reached, the slope of the neighboring path is directed toward the nominal in an effort to meet the terminal constraint.

Observing that $H_{\theta\theta} = -1$ in (C-3), it seems possible that increasing θ might minimize $\delta^2 J$. In fact, a necessary condition for the existence of a conjugate point is that $H_{\theta\theta} < 0$.

The following similarities between this simple problem and the re-entry problem are: (a) The feedback gains tabulated in Fig. 4 become positive at the beginning of the flight; (b) $-C = H_{xx} - H_{xu} H_{uu}^{-1} H_{ux}$ of (32) was not semi-negative definite [5] (here the performance index is to be maximized), and (c) the sweep variable S became unbounded along the optimal trajectory for the constrained problem. The latter means that along this path there is a conjugate point for the problem maximizing velocity with no terminal constraints. These same things also occurred for the nominal trajectory of Ref. [1].
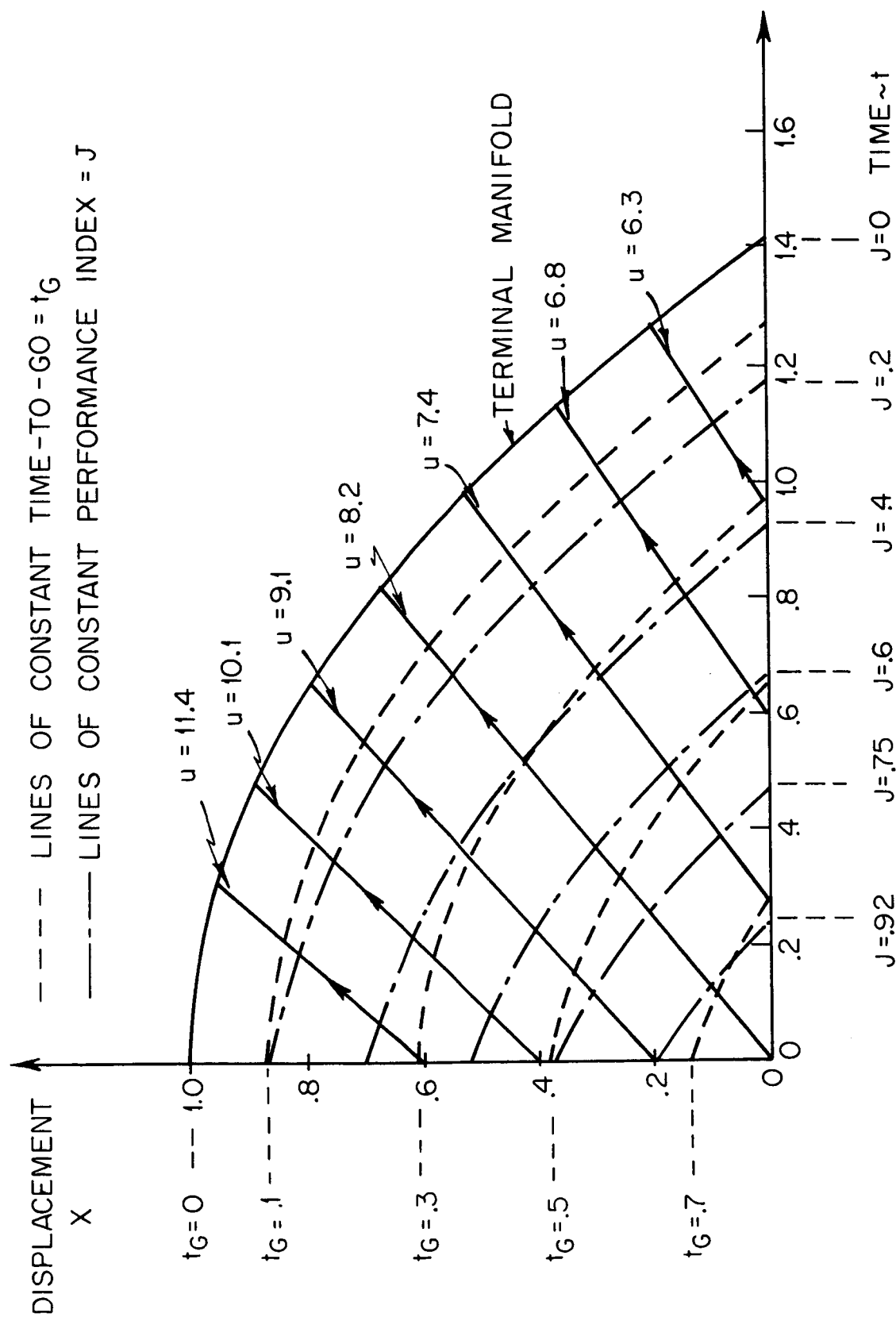
FIG. 1 TRAJECTORIES IN PURSUIT PROBLEM

LIFT

GLIDER ZERO-LIFT AXIS

α

VELOCITY = V

DRAG

γ (FLIGHT-PATH ANGLE)

WEIGHT

ALTITUDE = h

EARTH'S RADIUS
R

EARTH'S
SURFACE

SPACE-FIXED
REFERENCE
LINE

S = WING PLAN-FORM AREA

g_0 = GRAVITY AT SEA LEVEL

$g = g_0 \left(\dfrac{R}{Rth}\right)^2$ = LOCAL GRAVITY

m = MASS OF THE VEHICLE

W = mg = WEIGHT

C_L = LIFT COEF.

C_D = DRAG COEF.

$\rho(h)$ = ATMOSPHERIC DENSITY

$$LIFT = \frac{C_L \rho(h) V^2 S}{2}$$

$$DRAG = \frac{C_D \rho(h) V^2 S}{2}$$
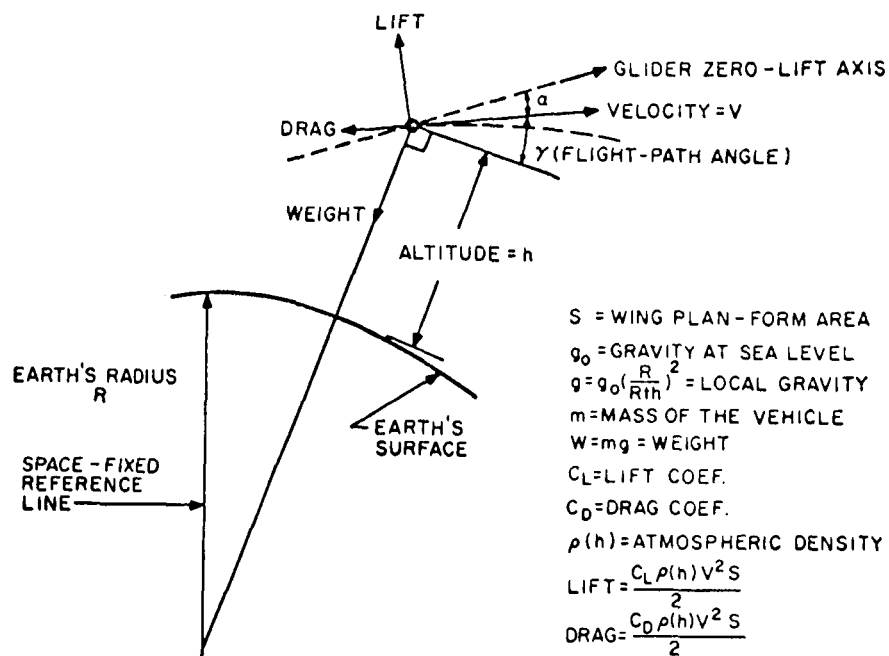
FIG. 2   GEOMETRY AND NOMENCLATURE OF ATMOSPHERIC
RE-ENTRY EXAMPLE PROBLEM.
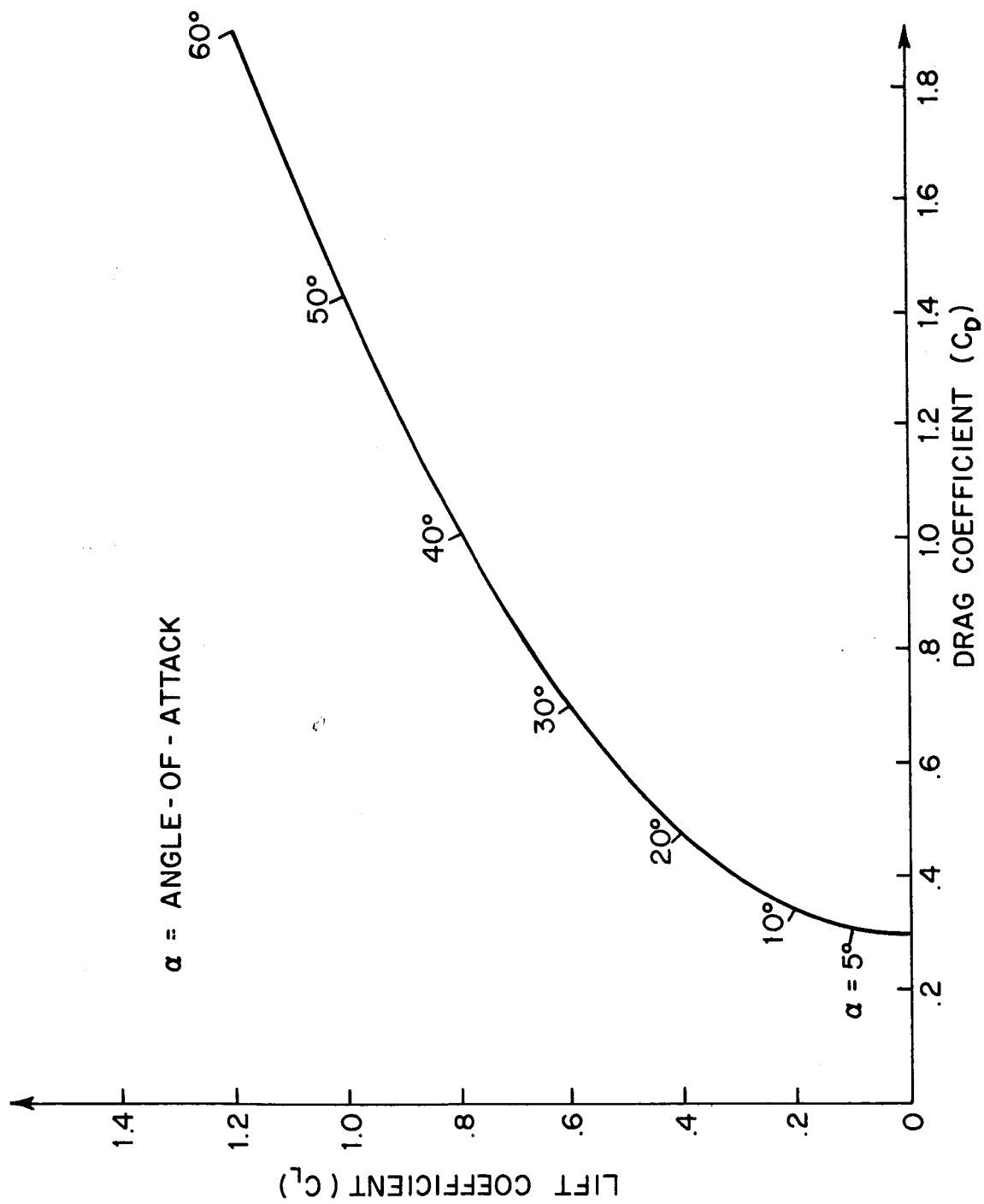
FIG. 3   LIFT-DRAG POLAR FOR RE-ENTRY VEHICLE

TIME	v	γ	h	α	$K_v^\alpha \times 10^3$	$K_\gamma^\alpha \times 10$	$K_h^\alpha \times 10^4$	$K_v^t \times 10^4$	$K_\gamma^t \times 10^2$	$K_h^t \times 10^3$
SEC	$\frac{FT}{SEC}$	RAD	FT	DEG	$\frac{DEG}{FT/SEC}$	$\frac{DEG}{RAD}$	$\frac{DEG}{FT}$	$\frac{SEC}{FT/SEC}$	$\frac{SEC}{RAD}$	$\frac{SEC}{FT}$
0	33961	-.0274	189890	32.41	.796	- .030	1.241	-18.08	-.302	- .398
5	33099	-.0018	187548	23.05	.405	- .044	- .843	-16.63	-.289	- .564
10	32504	.0159	188818	13.81	.016	- .059	-3.639	-15.24	-.285	- .718
15	32101	.0258	192280	5.49	-.348	- .078	-6.947	-13.90	-.292	- .869
20	31798	.0296	196770	-1.65	-.679	- .101	-10.837	-12.60	-.307	-1.031
25	31537	.0297	201498	-7.67	-.977	- .129	-15.71	-11.29	-.325	-1.22
30	31293	.0275	206008	-12.78	-1.248	- .166	-22.43	- 9.93	-.346	-1.45
35	31056	.0242	210048	-17.18	-1.494	- .215	-32.92	- 8.499	-.366	-1.75
40	30823	.0202	213485	-21.07	-1.720	- .287	-51.73	- 6.976	-.383	-2.18
45	30588	.0158	216248	-24.63	-1.830	- .402	-92.23	- 5.358	-.397	-2.89
50	30347	.0110	218288	-28.00	-1.903	- .628	-209.19	- 3.648	-.406	-4.27
55	30097	.0058	219559	-31.28	-1.971	-1.291	-852.45	- 1.858	-.409	-8.39
60	29827	-.0000	220000	-34.60	-1.990	∞	$-\infty$	- .188	-.408	∞

$$\delta\alpha = K_v^\alpha \delta v + K_\gamma^\alpha \delta\gamma + K_h^\alpha \delta h$$

$$\delta t_f = K_v^t \delta v + K_\gamma^t \delta\gamma + K_h^t \delta h$$

FIG. 4 TABLE OF STATE VARIABLE HISTORIES FOR THE NOMINAL MAXIMUM VELOCITY PATH, GAINS FOR INFLIGHT PREDICTION OF THE ERROR IN TIME-TO-GO, AND FEEDBACK GAINS.
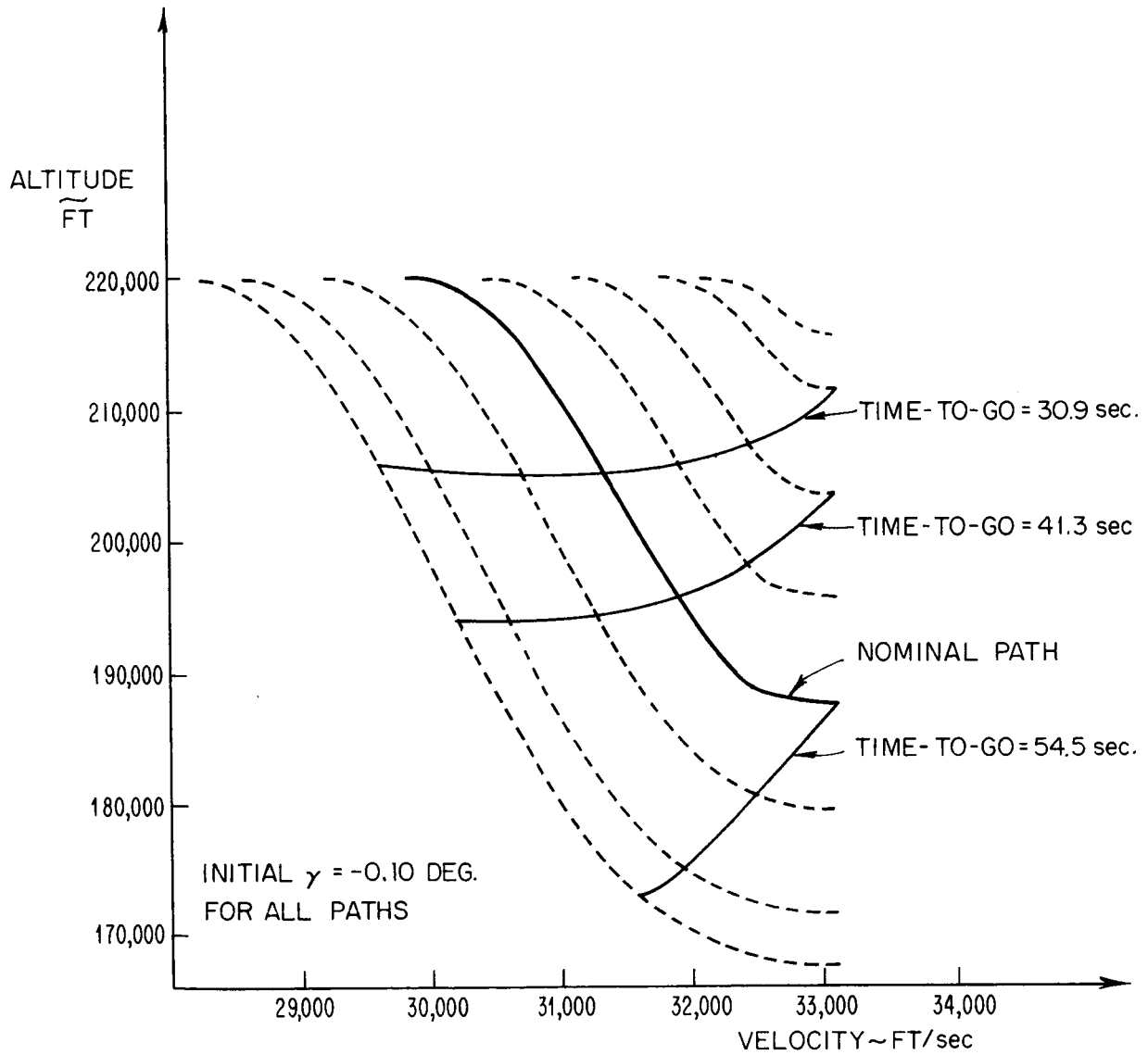
FIG. 5 TRAJECTORIES GENERATED BY MODIFIED NEIGHBORING
OPTIMUM CONTROL SCHEME DUE TO INITIAL ALTITUDE
PERTURBATIONS.
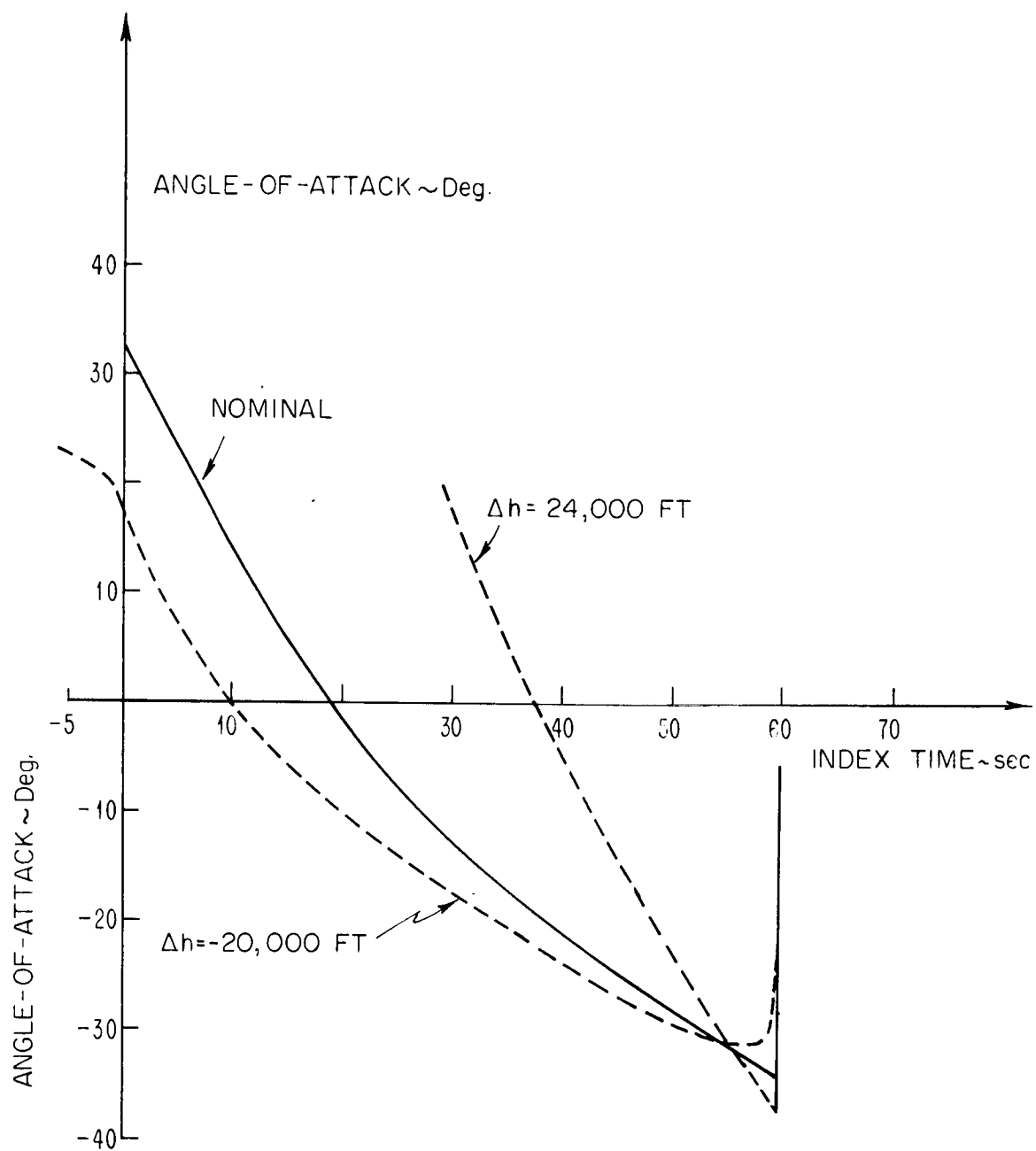
FIG. 6 ANGLE-OF-ATTACK PROGRAMS FOR NOMINAL PATH
OF A RE-ENTRY VEHICLE AND TWO PERTURBED PATHS.

INITIAL γ = -0.1 DEG.

NOMINAL PATH

ΔV = -10,000 ft/sec

ΔV = 13,000 ft/sec

ALTITUDE ~ FT

220,000
210,000
200,000
190,000
180,000

20,000   25,000   30,000   35,000   40,000   45,000   50,000

VELOCITY ~ FT/sec.
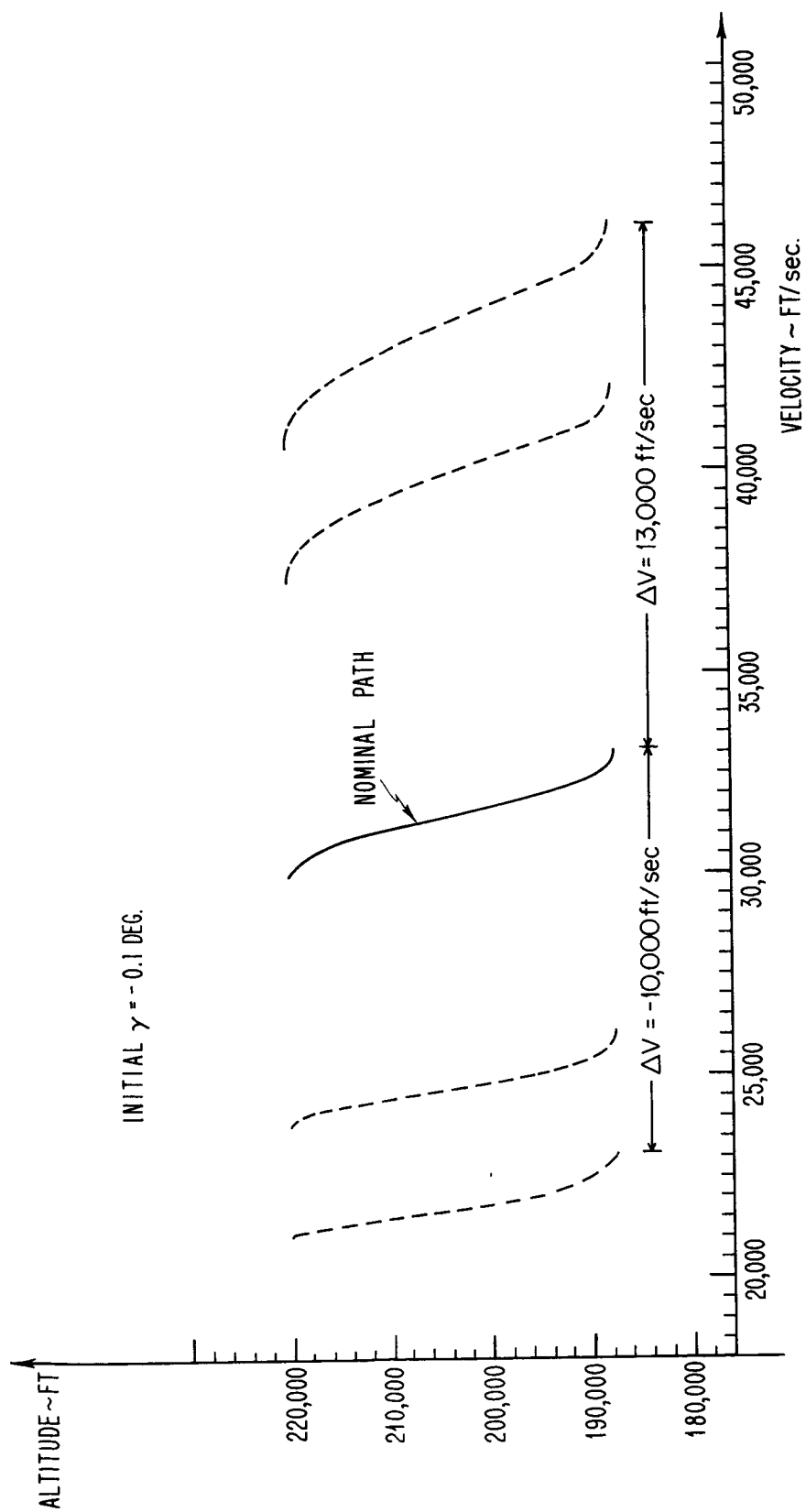
FIG. 7   TRAJECTORIES GENERATED BY MODIFIED NEIGHBORING OPTIMUM CONTROL SCHEME DUE TO INITIAL
VELOCITY PERTURBATIONS
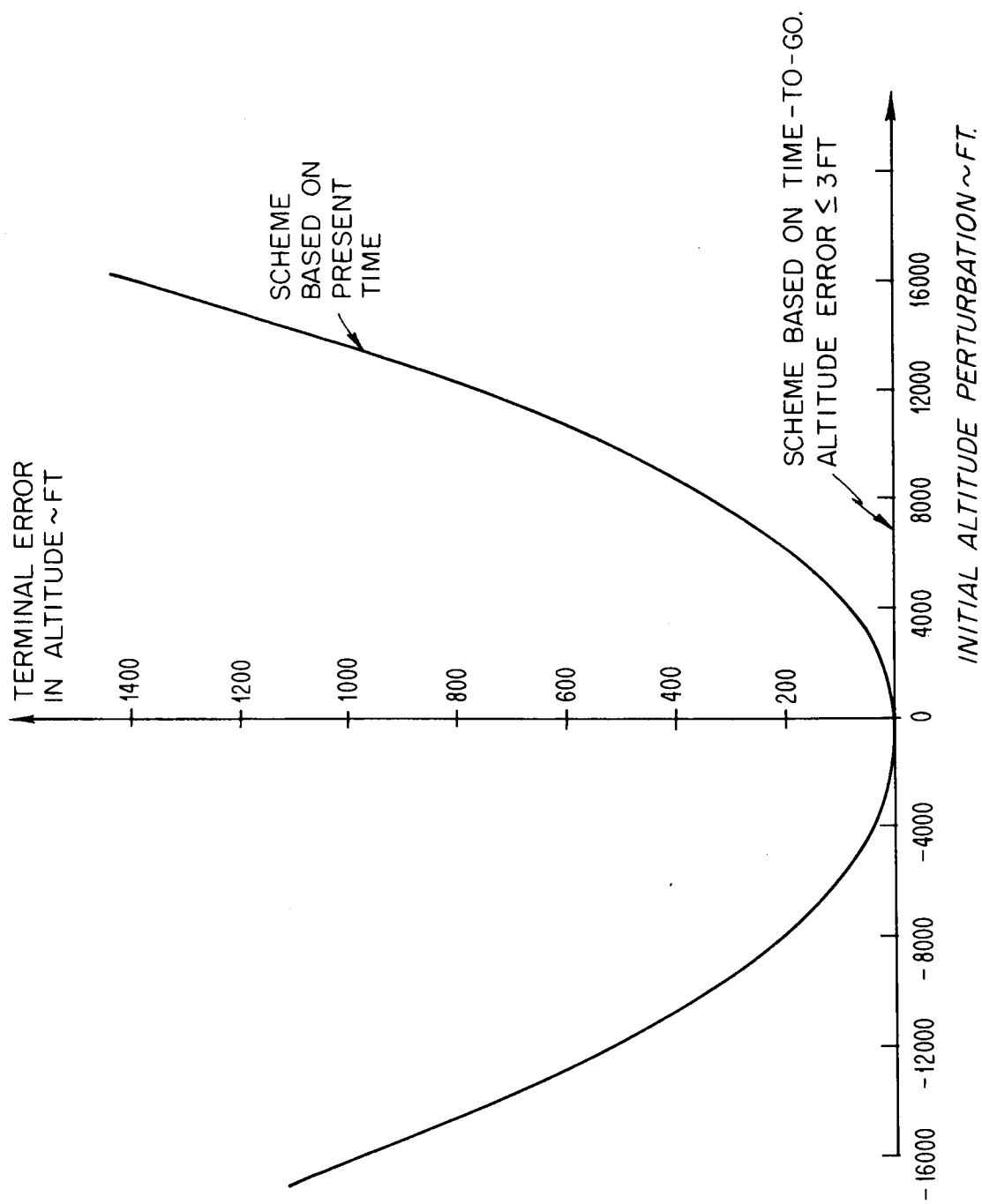
FIG. 8 TERMINAL ERROR IN ALTITUDE DUE TO INITIAL ALTITUDE PERTURBATIONS FOR CONTROL SCHEMES BASED ON TIME-TO-GO AND CLOCK TIME

ERROR IN TERMINAL ALTITUDE~FT

3000.

2000.

1000.

SCHEME
BASED ON
CLOCK TIME

SCHEME BASED ON
TIME-TO-GO

-10,000 -8,000 -6,000 -4,000 -2,000 0 2,000 4,000 6,000 8,000 10,000 12,000

INITIAL VELOCITY PERTURBATIONS~FT/sec.
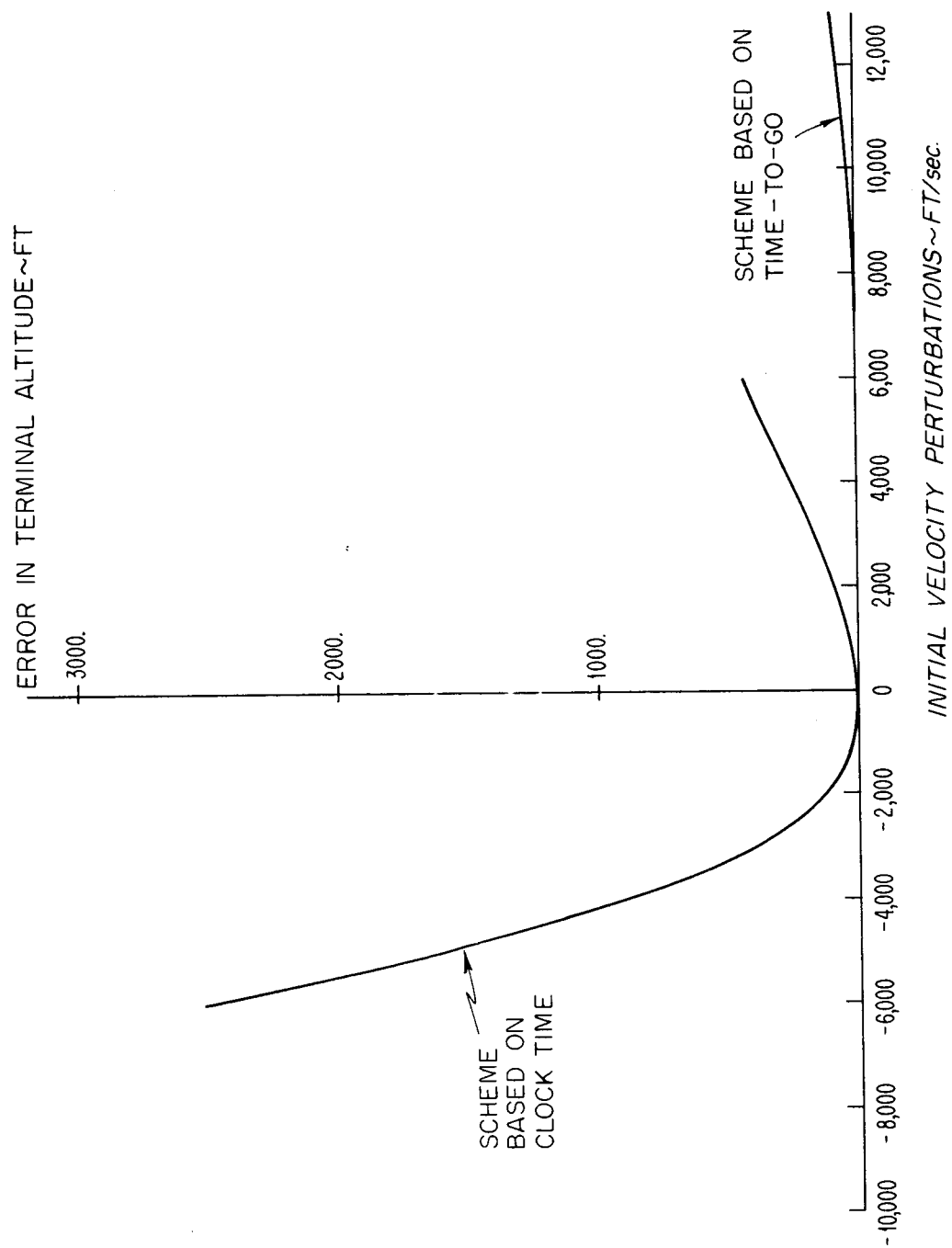
FIG. 9 TERMINAL ERROR IN ALTITUDE DUE TO INITIAL VELOCITY PERTURBATIONS FOR
CONTROL SCHEME BASED ON TIME-TO-GO AND CLOCK TIME.
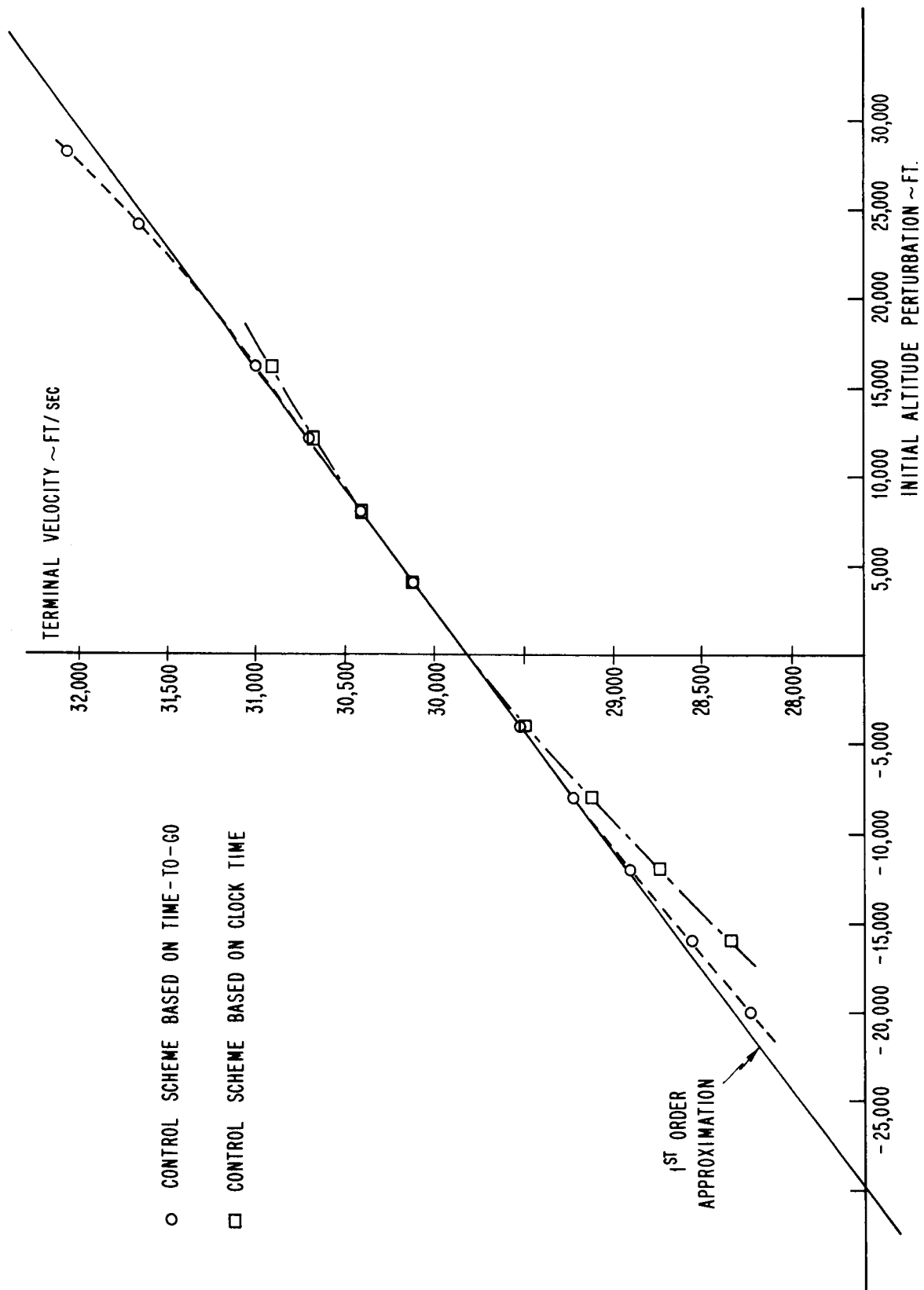
FIG. 10 TERMINAL VELOCITY COMPARISON OF CONTROL SCHEME BASED ON TIME-TO-GO AND CLOCK TIME.
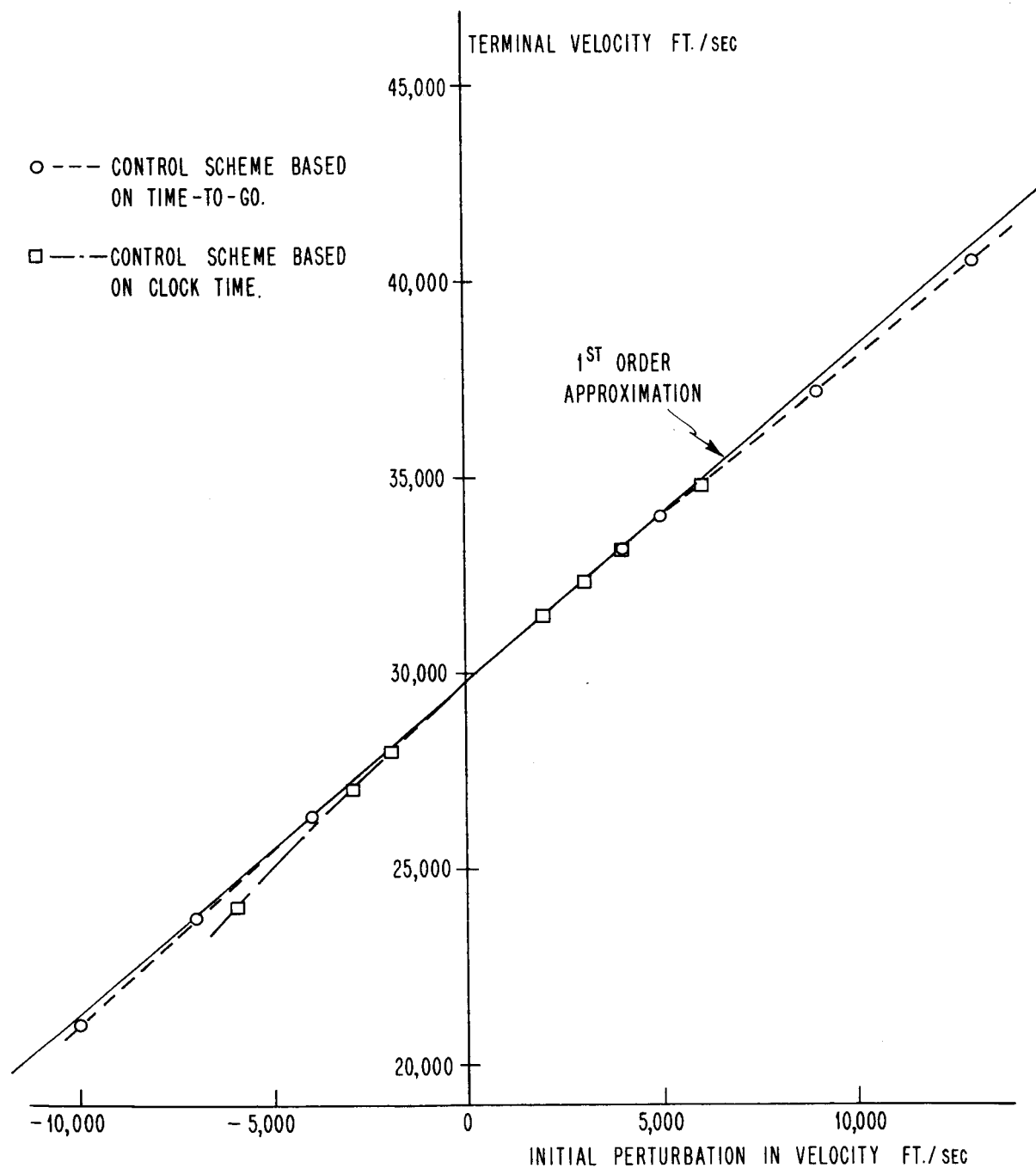
FIG. 11 TERMINAL VELOCITY COMPARISON OF CONTROL SCHEMES BASED ON TIME-TO-GO AND CLOCK TIME FOR INITIAL VELOCITY PERTURBATIONS.

MERIDIAN $\phi = \dfrac{\pi}{2}$

NEIGHBORING PATH

$\begin{cases} \theta = 0 \\ \phi = \pi \end{cases}$

NOMINAL PATH
($\theta(\phi) = 0$, EQUATOR)

FIG. 12   GEOMETRY FOR SHORTEST ARCS ON A
         SPHERE PROBLEM

Academy Library (DFSLB)
U. S. Air Force Academy
Colorado Springs, Colorado 80912

AEDC (ARO, INC)
Attn: Library/Documents
Arnold AFS, Tenn 37389

Aeronautics Library
Graduate Aeronautical Laboratories
California Institute of Technology
1201 E. California Blvd.
Pasadena, California 91109

Aerospace Corporation
P. O. Box 95085
Los Angeles, Calif 90045
Attn: Library Acquisitions Group

Airborne Instruments Laboratory
Deerpark, New York 11729

AFAL (AVTE/ R.D. Larson)
Wright-Patterson AFB
Ohio 45433

AFCRL (CRMXLR)
AFCRL Research Library, Stop 29
L. G. Hanscom Field
Bedford, Mass. 01731

AFETR (ETLLG-1)
STINFO Officer (for library)
Patrick AFB, Florida 32925

AFETR Technical Library
(ETV, MU-135)
Patrick AFB, Florida 32925

AFFTC (FTBPP-2)
Technical Library
Edwards AFB, California 93523

APGC (PHBPS-12)
Eglin AFB
Florida 32542

ARL (ARZY)
Wright-Patterson AFB
Ohio 45433

AUL3T-9663
Maxwell AFB
Alabama 36112

Mr. Henry L. Bachmann
Assistant Chief Engineer
Wheeler Laboratories
122 Cuttermill Road
Great Neck, New York 11021

Bendix Pacific Division
11600 Sherman Way
North Hollywood, California 91605

Colonel A. D. Blue
RTD (RTTL)
Bolling Air Force Base, D. C. 20332

California Institute of Technology
Pasadena, California 91109
Attn: Documents Library

Carnegie Institute of Technology
Electrical Engineering Dept.
Pittsburgh, Pa 15213

Central Intelligence Agency
Attn: OCR/DD Publications
Washington, D. C. 20505

Chief of Naval Operations
OP-07
Washington, D. C. 20350

Chief of Naval Research
Department of the Navy
Washington, D. C. 20360
Attn: Code 427

Commandant
U. S. Army and General Staff College
Attn: Secretary
Fort Leavenworth, Kansas 66270

Commander
Naval Air Development and
Material Center
Johnsville, Pennsylvania 18974

Commanding General
Frankford Arsenal
Attn: SMUFA-L6000 (Dr. Sidney Ross)
Philadelphia, Pa. 19137

Commandant
U. S. Army Air Defense School
Attn: Missile Sciences Div. C & S Dept.
P. O. Box 9390
Fort Bliss, Texas 79916

Commander
U. S. Naval Air Missile Test Center
Point Mugu, California 93041

Commanding General
Attn: STE 5-S-VT
White Sands Missile Range
New Mexico 88002

Commanding General
U. S. Army Electronics Command
Fort Monmouth, New Jersey 07703

Attn: AMSEL-SC
RD-D
RD-G
RD-GF
RD-MAT
XL-D
XL-E
XL-C
XL-S
NL-D
NL-CT-R
HL-CT-P
HL-CT-L
HL-CT-O
HL-CT-I
HL-CT-A
NL-D
KL-A
NL-P
NL-R
NL-S
KL-D
KL-E
KL-S
KL-T
VL-D
WL-D

Commanding General
U. S. Army Material Command
Attn: AMCRD-RS-DE-Z
Washington, D. C. 20315

Commanding General
U. S. Army Missile Command
Attn: Technical Library
Redstone Arsenal, Alabama 35809

Commanding Officer
Naval Avionics Facility
Indianapolis, Indiana 46241

Commanding Officer
Naval Ordnance Laboratory
Corona, California 91720

Commanding Officer
Naval Ordnance Laboratory
White Oak, Maryland 21502

Commanding Officer
Naval Ordnance Test Station
China Lake, California 93555

Commanding Officer
Naval Training Device Center
Orlando, Florida 32811

Commanding Officer
Office of Naval Research Branch Office
1030 East Green Street
Pasadena, California

Commanding Officer
Office of Naval Research Branch Office
219 South Dearborn Street
Chicago, Illinois 60604

Commanding Officer
Office of Naval Research Branch Office
495 Summer Street
Boston, Massachusetts 02210

Commanding Officer
Office of Naval Research Branch Office
207 West 24th Street
New York, New York 10011

Commanding Officer
Office of Naval Research Branch Office
Box 39, Navy No. 100 F. P. O.
New York, New York 09510

Commanding Officer
U. S. Army Electronics R & D Activity
Fort Huachuca, Arizona 85163

Commanding Officer
U. S. Army Electronics R & D Activity
White Sands Missile Range
New Mexico 88002

Commanding Officer
U. S. Army Engineer R & D Laboratory
Attn: STINFO Branch
Fort Belvoir, Virginia 22060

Commanding Officer
U. S. Army Research Office (Durham)
Attn: CRD-AA-IP (Richard O. Ulsh)
Box CM, Duke Station
Durham, North Carolina 27706

Commanding General
U. S. Army Strategic Communications
Command
Washington, D. C. 20315

Commanding Officer
Harry Diamond
Attn: Dr. Berthold Altman (AMXDO-TI)
Connecticut Avenue & Van Ness Street NW
Washington, D. C. 20438

Commanding Officer
Human Engineering Laboratories
Aberdeen Proving Ground, Maryland 21005

Commanding Officer
U. S. Army Ballistics Research Laborat.
Attn: V. W. Richards
Aberdeen Proving Ground
Aberdeen, Maryland 21005

Commanding Officer
U. S. Army Limited War Laboratory
Attn: Technical Director
Aberdeen Proving Ground
Aberdeen, Maryland 21005

Commanding Officer
U. S. Army Materials Research Agency
Watertown Arsenal
Watertown, Massachusetts 02172

Commanding Officer
U. S. Army Security Agency
Arlington Hall
Arlington, Virginia 22212

Commanding Officer and Director
U. S. Naval Underwater Sound Lab.
Fort Trumbull
New London, Connecticut 06840

Defense Documentation Center
Attn: TISIA
Cameron Station, Bldg. 5
Alexandria, Virginia 22314

Det #6, OAR (LODAR)
Air Force Unit Post Office
Los Angeles, Calif. 90045

Director
Advanced Research Projects Agency
Department of Defense
Washington, D. C. 20301

Director for Materials Sciences
Advanced Research Projects Agency
Department of Defense
Washington, D. C. 20301

Director
Columbia Radiation Laboratory
Columbia University
538 West 120th Street
New York, New York 10027

Director
Coordinated Science Laboratory
University of Illinois
Urbana, Illinois 61803

Director
Electronics Research Laboratory
University of California
Berkeley, California 94720

Director
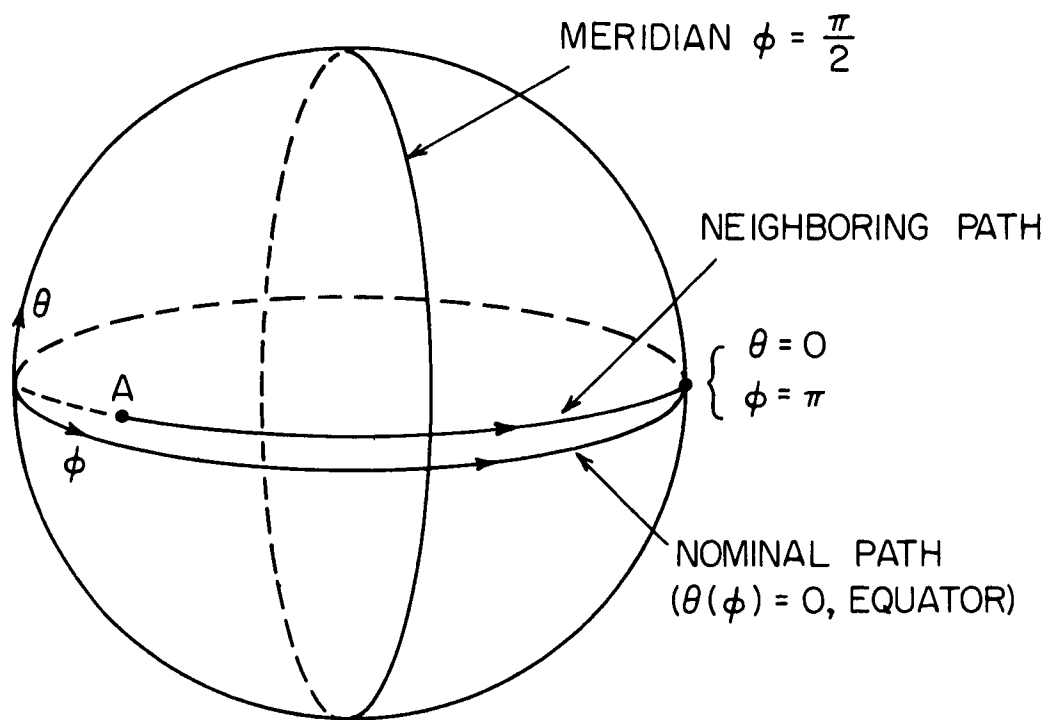Electronic Sciences Laboratory
University of Southern California
Los Angeles, California 90007

Director
Microwave Laboratory
Stanford University
Stanford, California 94305

Director - Inst. for Exploratory
Research
U. S. Army Electronics Command
Attn: Mr. Robert O. Parker, Executive
Secretary, JSTAC (AMSEL-XL-D)
Fort Monmouth, New Jersey 07703

Director
National Security Agency
Attn: Librarian C-332
Fort George G. Meade, Maryland 20755

Director, Naval Research Laboratory
Technical Information Officer
Washington, D. C.
Attn: Code 2000

Director
Research Laboratory of Electronics
Massachusetts Institute of Technology
Cambridge, Mass. 02139

Director
Stanford Electronics Laboratories
Stanford University
Stanford, California 94305

Director, USAF Project RAND
Via: Air Force Liaison Office
The RAND Corporation
1700 Main St., Santa Monica, Cal. 90406
Attn: Library

Director
U. S. Army Engineer Geodesy,
Intelligence and Mapping
Research and Development Agency
Fort Belvoir, Virginia 22060

Director
U. S. Naval Observatory
Washington, D. C. 20390

Director, U. S. Naval Security Group
Attn: G43
3801 Nebraska Avenue
Washington, D. C. 20390

Division of Engineering and Applied
Physics
210 Pierce Hall
Harvard University
Cambridge, Massachusetts 02138

Professor A. A. Dougal, Director
Laboratories for Electronics and
Related Sciences Research
University of Texas
Austin, Texas 78712

ESD (ESTI)
L. G. Hanscom Field
Bedford, Mass. 01731

European Office of Aerospace Research
Shell Building
47 Rue Cantersteen
Brussels, Belgium

Colonel Robert E. Fontana
Department of Electrical Engineering
Air Force Institute of Technology
Wright-Patterson AFB, Ohio 45433

General Electric Co.
Research Laboratories
Schenectady, New York 12301

Professor Nicholas George
California Inst. of Technology
Pasadena, California 91109

Dr. H. V. Noble
Air Force Avionics Laboratory
Wright-Patterson AFB, Ohio 45433

Goddard Space Flight Center
National Aeronautics and Space Admin.
Attn: Library, Documents Section
Code 252
Green Belt, Maryland 20771

Dr. John C. Hancock, Director
Electronic Systems Research Laboratory
Purdue University
Lafayette, Indiana 47907

Dr. H. Harrison, Code RRE
Chief, Electrophysics Branch
National Aeronautics and Space
Administration
Washington, D. C. 20546

Head, Technical Division
U. S. Naval Counter Intelligence
Support Center
Fairmont Building
4420 North Fairfax Drive
Arlington, Virginia 22203

Headquarters
Defense Communications Agency
The Pentagon
Washington, D. C. 20305

Dr. L. M. Hollingsworth
AFCRL (CRN)
L. G. Hanscom Field
Bedford, Massachusetts 01731

Hunt Library
Carnegie Institute of Technology
Schenley Park
Pittsburgh, Pa. 15213

The Johns Hopkins University
Applied Physics Laboratory
8621 Georgia Avenue, Silver Spring, Md.
Attn: Boris H. Kuvshinoff   20910
Document Librarian

Lt. Col Robert B. Kalisch
Chief, Electronics Division
Directorate of Engineering Sciences
Air Force Office of Scientific Research
Arlington, Virginia 22209

Colonel Kee
AFRSTE
Hqs. USAF
Room ID-429, The Pentagon
Washington, D. C. 20330

Dr. S. Benedict Levin, Director
Institute for Exploratory Research
U. S. Army Electronics Command
Fort Monmouth, New Jersey 07703

Los Alamos Scientific Laboratory
Attn: Reports Library
P. O. Box 1663
Los Alamos, New Mexico 87544

Librarian
U. S. Naval Electronics Laboratory
San Diego, California 95152

Librarian
U. S. Navy Post Graduate School
Monterey, California 93940

Lockheed Aircraft Corp
P. O. Box 504
Sunnyvale, California 94088

Dr. I. R. Mirman
AFSC (SCT)
Andrews Air Force Base, Maryland 20331

Lt. Col Bernard S. Morgan
Frank J. Seiler Research Laboratory
U. S. Air Force Academy
Colorado Springs, Colorado 60912

Dr. G. J. Murphy
The Technological Institute
Northwestern University
Evanston, Illinois 60201

Mr. Peter Murray
Air Force Avionics Laboratory
Wright-Patterson AFB, Ohio 45433

NASA Lewis Research Center
Attn: Library
21000 Brookpark Road
Cleveland, Ohio 44135

NASA Scientific & Technical
Information Facility
Attn: Acquisitions Branch (S/AK/DL)
P. O. Box 33
College Park, Maryland 20740

National Science Foundation
Attn: Dr. John R. Lehmann
Division of Engineering
1800 G Street, N. W.
Washington, D. C. 20550

National Security Agency
Attn: R4-James Tippet
Office of Research
Fort George G. Meade, Maryland 20755

Naval Air Systems Command
AIR 03
Washington, D. C. 20360

Naval Electronics Systems Command
ELEX 03
Falls Church, Virginia 22046

Naval Ordnance Systems Command
ORD 32
Washington, D. C. 20360

Naval Ordnance Systems Command
SHIP 035
Washington, D. C. 20360

Naval Ship Systems Command
SHIP 031
Washington, D. C. 20360

New York University
College of Engineering
New York, New York 10019

Office of Deputy Director
(Research and Information Rm. 3D1087)
Department of Defense
The Pentagon
Washington, D. C. 20301

Polytechnic Institute of Brooklyn
55 Johnson Street
Brooklyn, New York 11201
Attn: Mr. Jerome Fox
Research Coordination

RADC (EMLAL-1)
Griffiss AFB, New York 13442
Attn: Documents Library

Raytheon Co
Bedford, Mass. 01730
Attn: Librarian

Lt. Col. J. L. Reeves
AFSC (SCBB)
Andrews Air Force Base, Md 20331

Dr. Edward M. Reilley
Asst. Director (Research)
Offc. of Defense Res. & Eng.
Department of Defense
Washington, D. C. 20301

Research Plans Office
U. S. Army Research Office
3045 Columbia Pike
Arlington, Virginia 22204

Dr. H. Robl, Deputy Chief Scientist
U. S. Army Research Office (Durham)
Durham, North Carolina 27706

Emil Schafer, Head
Electronics Properties Info Center
Hughes Aircraft Co
Culver City, California 90230

School of Engineering Sciences
Arizona State University
Tempe, Arizona 85281

Space Systems Division
Air Force Systems Command
Los Angeles Air Force Station
Los Angeles, California 90045
Attn: SSSD

SSD (SSTRT/Lt. Starbuck)
AFUPO
Los Angeles, California 90045

Superintendent
U. S. Army Military Academy
West Point, New York 10996

Colonel A. Swan
Aerospace Medical Division
Brooks Air Force Base, Texas 78235

Syracuse University
Department of Electrical Engineering
Syracuse, New York 13210

Systems Engineering Group (RTD)
Technical Information Reference Branch
Attn: SEPIR
Direct. of Eng. Stand & Tech. Inf.
Wright-Patterson AFB, Ohio 45433

University of California
Santa Barbara, California 93106
Attn: Library

University of California at Los Angeles
Department of Engineering
Los Angeles, California 90024

University of Michigan
Electrical Engineering Dept.
Ann Arbor, Michigan 48104

U. S. Army Munitions Command
Attn: Technical Information Branch
Picatinney Arsenal
Dover, New Jersey 07801

U. S. Army Research Office
Attn: Physical Sciences Division
3045 Columbia Pike
Arlington, Virginia 22204

U. S. Atomic Energy Commission
Division of Technical Information Ext.
P. O. Box 62
Oak Ridge, Tenn. 37831

U. S. Naval Weapons Laboratory
Dahlgren
Virginia 22448

Major Charles Waespy
Technical Division
Deputy for Technology
Space Systems Division, AFSC
Los Angeles, California 90045

The Walter Reed Institute of Research
Walter Reed Medical Center
Washington, D. C. 20012

Colonel J. D. Warthman
AFSC (SCTR)
Andrews Air Force Base, Maryland 20331

Weapons Systems Test Division
Naval Air Test Center
Patuxtent River, Maryland 20670
Attn: Library

Weapons Systems Evaluation Group
Attn: Col. Daniel W. McElwee
Department of Defense
Washington, D. C. 20305

Yale University
Engineering Department
New Haven, Connecticut 06720

Mr. Charles F. Yost
Special Assistant to the Director of
Research
National Aeronautics and Space Admin.
Washington, D. C. 20546

Dr. Leo Young
Stanford Research Institute
Menlo Park, California 94025

DOCUMENT CONTROL DATA - R & D

Security classification of title, body of abstract and indexing annotation must be entered when the overall report is classified)

1. ORIGINATING ACTIVITY (Corporate author)	2a. REPORT SECURITY CLASSIFICATION
Division of Engineering and Applied Physics Harvard University Cambridge, Massachusetts	Unclassified
	2b. GROUP

3. REPORT TITLE

A NEIGHBORING OPTIMUM FEEDBACK CONTROL SCHEME BASED ON ESTIMATED TIME-TO-GO WITH APPLICATION TO RE-ENTRY FLIGHT PATHS

4. DESCRIPTIVE NOTES (Type of report and inclusive dates)

Interim technical report

5. AUTHOR(S) (First name, middle initial, last name)

Jason L. Speyer and Arthur E. Bryson, Jr.

6. REPORT DATE	7a. TOTAL NO. OF PAGES	7b. NO. OF REFS
June 1967	47	5

8a. CONTRACT OR GRANT NO. Nonr-1866(16) and NASA Grant NGR 22-007-068	9a. ORIGINATOR'S REPORT NUMBER(S)
b. PROJECT NO.	Technical Report No. 527
c.	9b. OTHER REPORT NO(S) (Any other numbers that may be assigned this report)
d.	

10. DISTRIBUTION STATEMENT

Reproduction in whole or in part is permitted by the U. S. Government. Distribution of this document is unlimited.

11. SUPPLEMENTARY NOTES	12. SPONSORING MILITARY ACTIVITY
	Office of Naval Research

13. ABSTRACT

A modification of the perturbation feedback control scheme of Refs. [1], [2], and [3] is presented that greatly increases its capability to handle disturbances in cases where the final time is not specified. The modified control scheme uses a set of precalculated gains which allows in-flight estimation of the change in the final time due to perturbations from a nominal path. The time-to-go, determined from the predicted change in final time, is used to enter tables of precalculated feedback control gains.

This modified guidance scheme is applied to a re-entry glider entering the atmosphere of the Earth at supercircular velocities. Beginning at the bottom of the pull-up maneuver (nominal altitude 188,000 ft., nominal velocity 33,000 ft./sec. $^{-1}$) the glider is guided to a terminal altitude of 220,000 ft. and zero (0) flight path angle with maximum terminal velocity. For initial altitudes between 167,000 and 216,000 ft. the terminal error in altitude is less than two feet; for initial velocities between 23,000 ft./sec. and 43,000 ft./sec. the terminal altitude error is less than 13 ft. In addition, the terminal velocity is very close to optimal for these initial conditions.

The suggestion for using such a scheme was first given by Kelley [4] who used performance index-to-go as the index variable. He called this a "transversal comparison" scheme. Time-to-go has the advantage that it always decreases monotonically whereas this is not always true of performance index-to-go. A monotonically changing index variable must be used if the transversal comparisons are to be made over the entire flight. The transversal comparison is used here in an iterative scheme to predict the time-to-go. Kelley's suggestion is also extended to include non-stationary systems and in-flight changes in the terminal constraints.

DD FORM 1473 (PAGE 1)
1 NOV 65
S/N 0101-807-6811

A-31408

14. KEY WORDS	LINK A		LINK B		LINK C	
	ROLE	WT	ROLE	WT	ROLE	WT
optimum feedback control scheme						
estimated time-to-go						
re-entry flight paths						

DD `FORM 1 NOV 65` **1473** (BACK)

S/N 0101-807-6821